

Repairing the Injured Spinal Cord using Pleiotrophin and Rehabilitative Training

by

Carmen Ng

A thesis submitted in partial fulfillment of the requirements for the degree of

Master of Science

Neuroscience

University of Alberta

© Carmen Ng, 2023

Abstract:

Background: Functional recovery following a spinal cord injury (SCI) is linked to neuroplasticity, including neurite outgrowth and rewiring of neuronal connections rostral and caudal to the injury. Plasticity promoting treatments can be targeted to specific locations within the central nervous system (CNS) to encourage functional recovery and minimize side effects such as pain or spasticity caused by aberrant or unwanted connections. However, the optimal location(s) to promote beneficial plasticity have not yet been identified which poses a significant translational challenge.

My research explores the use of pleiotrophin (PTN) as a neuroplasticity promoting treatment. PTN is an endogenously occurring growth factor with a unique dual nature that neutralizes growth inhibitory chondroitin sulfate proteoglycan (CSPGs) and upregulates growth promoting pathways within neurons. To develop PTN as a plasticity promoting treatment, my thesis aimed to identify a dose of PTN that would maximize neurite outgrowth from the corticospinal tract (CST), to determine which location(s) of PTN administration (e.g., rostral or caudal of an SCI) would encourage the most functional recovery, and to assess whether PTN treatment combined with rehabilitative training would elicit a complementary effect on functional recovery.

Methodology: PTN was applied onto cortical cell cultures grown on CSPGs at concentrations of 1.25 $\mu\text{g}/\text{mL}$ or 10 $\mu\text{g}/\text{mL}$ to ensure our supply of PTN could promote neurite outgrowth at a level similar to published studies. The efficacy of our PTN was also screened using *in vivo* rat models of SCI and compared to chondroitinase ABC (ChABC), an alternative plasticity promoting treatment that acts only by digesting CSPGs. PTN and ChABC was administered into the intermediate grey matter of the spinal cord to target CSPGs within the perineuronal network

(PNN) that act to stabilize neuronal connections. To identify the optimal dose of PTN, an *in vivo* dose-response experiment was conducted using a C4 dorsolateral quadrant (DLQ) rat model of SCI. Neurite outgrowth from the CST was compared between rats receiving different concentrations of PTN treatment and between male and female rats for any potential sex differences. We then used a contusion model of SCI to assess the effects of PTN treatment targeted to different locations in the spinal cord. PTN treatment was targeted bilaterally rostral and caudal to the SCI into the intermediate grey matter of the spinal cord. Targeted PTN treatment was combined with rehabilitative training using the single pellet grasping (SPG) task as a measure of functional recovery. Following the contusion model, a DLQ model of SCI was used to assess the effects of PTN treatment targeted into the intermediate grey matter ipsilesional and caudal to the SCI. PTN treatment was also combined with SPG training to assess functional recovery in PTN treated rats compared to PBS treated SCI rats.

Principal Findings: Our results indicate that different concentrations of PTN elicit different extents of neurite outgrowth and PTN induced neurite outgrowth may differ between sexes. PTN treatment targeted to different locations in the spinal cord did not alter the quantity of midline crossing fibers rostral or caudal to the SCI compared to PBS treated rats. Paradoxically, PTN treated rats performed worse than PBS treated rats in the SPG task in both the contusion and DLQ models of SCI. There may be several factors contributing to the difference in SPG performance between PTN and PBS treated rats. Firstly, it could be that PTN treatment induces tissue damage that was not detected from our methods of histological analysis. Secondly, differences in SPG performance may be due to alterations in the neuronal circuitry controlling sensory signalling in PTN treated rats. Lastly, PTN treated rats had less synaptic density in the

ventral horn of the spinal cord potentially indicating a decrease in neuronal connections controlling motor function.

Conclusions: PTN can influence neuroplasticity and functional outcomes following a SCI. However, further investigation is needed to elucidate the exact anatomical changes underlying the worse functional outcomes in PTN treated rats.

Preface:

Research ethics for all research projects a part of this thesis was approved by the University of Alberta Health Sciences Ethics Board, Project Name “Repairing the Injured Spinal Cord”, No. AUP 00000254, 7/1/2019-6/30/2022. The majority of the work presented in this thesis is the original work of Carmen Ng. Some of the research presented in this thesis was completed with the help of a laboratory technician, Kiera Smith, an undergraduate student, Kayle Lowe, and a PhD student, Somnath Gupta. Kiera Smith assisted with daily animal care and the care of animals during and following all surgical procedures in each experiment conducted for my thesis except for the *PTN Dose-Response* experiment. Kiera Smith also trained the rats in the SPG task for the *SPG DLQ SCI* experiment and conducted the high-speed analysis for this experiment. Kayle Lowe and Kiera Smith completed the neurite outgrowth and bassoon analysis for the *SPG DLQ SCI* experiment as a part of Kayle Lowe’s undergraduate neuroscience thesis project. Kayle Lowe presented this data in her undergraduate thesis. Lastly, the cell culture portion of the *PTN in vitro* experiment was completed by Somnath Gupta from the laboratory of Dr. I. Winship at the University of Alberta.

Acknowledgements:

I would like to acknowledge the Wings for Life Foundation for funding all of the projects included in this thesis. The grant proposal to Wings for Life was composed by my supervisors Keith Fenrich and Karim Fouad, and I would like to thank them both for allowing me to take the lead on this grant as a graduate student. The skill set, the knowledge, and the experiences they have taught and given me over the years will be carried with me as I continue my education and build my career. The work presented in my thesis was completed with the support of two laboratory technicians, Keira Smith, and Pamela Raposo. I would like to thank them for their incredible support and guidance over the past three years. It was a pleasure to have Dr. I Winship and Dr. C Webber on my supervisory committee and I would like to thank them for the support and resources they provided me over the course of my degree. Lastly, I would like to acknowledge the Neuroscience and Mental Health Institute (NMHI) for providing a cohesive and supportive learning environment throughout my degree and for nominating me for numerous scholarships throughout my degree. The contribution of each individual and the NMHI throughout my degree was crucial to my success in completing my graduate degree.

Table of Contents:

Abstract:	ii
Preface:	v
Acknowledgements:	vi
Table of Contents:	vii
List of Figures:	x
Chapter 1: Introduction	1
1.1 Epidemiology of spinal cord injury (SCI).....	1
1.2 Pathophysiology of SCI	1
1.3 The development of pharmacological treatments to improve recovery following an SCI	4
1.4 Combinatorial pharmacological treatments	7
1.5 Rehabilitative treatment following SCI	8
1.6 Benefits of combining rehabilitative training with pharmacological treatments	10
1.7 Emergence of a new pharmacological treatment to promote neurite outgrowth following an SCI..	11
Chapter 2: Methods	17
2.1 Animal Care and Ethics:	17
2.2 PTN and ChABC Preparation:	17
2.3 Cortical Cell Cultures:	19
2.3 Surgical Timing, Preparation, and Care:.....	21
2.4 SCI Surgeries:	22
2.5 PTN Spinal Injection Surgeries:	23
2.6 AAV9 CST Tracer Injection Surgeries:	26
2.7 Behavioural Testing:.....	27
2.8 Rehabilitative Training	29

2.9 Histological Analysis:.....	31
2.10 Immunohistochemistry:	32
2.11 Neurite Outgrowth and Synaptic Density Analysis:	34
2.12 Statistical Analysis:.....	36
Chapter 3: Results	37
3.1 PTN <i>in vitro</i> experiment: PTN promotes neurite outgrowth <i>in vitro</i>	37
3.2 PTN vs. ChABC experiment: PTN promotes neurite outgrowth at a similar level to neurite outgrowth induced by ChABC.....	37
3.3 PTN dose-response experiment: Higher doses of PTN may cause spinal cord damage.....	38
3.4 PTN dose-response experiment: PTN does not adversely alter forepaw sensation or long-term motor performance.....	39
3.5 PTN dose-response experiment: PTN-induced neurite outgrowth is dose-dependent and may differ between sexes.....	40
3.6 PTN contusion SCI experiment: PTN-treated rats performed worse than PBS-treated rats in the SPG task.....	41
3.7 PTN contusion SCI experiment: changes in midline crossing CST fibers did not correlate to the poorer SPG performance of PTN treated rats	42
3.8 PTN DLQ SCI experiment: PTN-treated rats with a DLQ SCI performed worse than PBS-treated rats in the SPG task	42
3.9 PTN DLQ SCI experiment: PTN-treated rats had more GFP traced CST fibres in the dorsal horn ipsilesional compared to CTRL rats.....	44
3.10 PTN DLQ SCI experiment: PTN-treated rats had less synaptic density in the VH compared to CTRL rats ipsilesional and caudal to the spinal injection site	45
Chapter 4: Discussion	47
4.1 PTN <i>in vitro</i> :	48
4.2 Application of PTN compared to ChABC <i>in vivo</i>	49

4.3 Dose-Response Experiment:	51
4.4 PTN Contusion SCI:	57
4.5 PTN DLQ SCI:	60
4.6 Bringing together the anatomical and functional data across PTN experiments:	63
4.7 Future Directions:	65
Chapter 5: Conclusion	66
Chapter 6: The Future of SCI research	66
Chapter 6: Figures	70
Figure 1: Schematics of rat SCI, spinal injections, and cortical injections for each experiment.	70
Figure 2: Application of PTN <i>in vitro</i>	71
Figure 3: PTN promotes neurite outgrowth in vivo.	74
Figure 4: Anatomical results from the PTN dose-response experiment.	75
Figure 5: Sensory and motor changes noted during the PTN dose-response experiment.	77
Figure 6: PTN dose-response heatmaps. analysis.	79
Figure 7: Outcome of rats with a contusion SCI treated with PTN and SPG training compared to PBS- treated rats.	80
Figure 8: Comparison of midline crossing fibres from PTN and PBS treated rats following the contusion SCI.	83
Figure 9: Outcome of rats with a DLQ SCI treated with PTN and SPG training compared to PBS- treated rats with SPG training.	84
Figure 10: Analysis of GFP and tdTom tracing intensity and synaptic density using bassoon IHC.	87
Bibliography	88

List of Figures:

Figure 1:	Page 70
Schematics of rat SCI, spinal injections, and cortical injections for each experiment	
Figure 2:	Page 71
Application of PTN <i>in vitro</i>	
Figure 3:	Page 73
PTN promotes neurite outgrowth <i>in vivo</i>	
Figure 4:	Page 75
Anatomical results from the PTN dose-response experiment	
Figure 5:	Page 77
Sensory and motor changes noted during the PTN dose-response experiment	
Figure 6:	Page 79
PTN dose-response heatmap analysis	
Figure 7:	Page 80
Outcome of rats with a contusion SCI treated with PTN and SPG training compared to PBS-treated rats	
Figure 8:	Page 82
Comparison of midline crossing fibres from PTN and PBS-treated rats following a contusion SCI	
Figure 9:	Page 84
Outcome of rats with a DLQ SCI treated with PTN and SPG training compared to CTRL rats with SPG training	
Figure 10:	Page 86
Analysis of GFP and tdTom tracing intensity and synaptic density using bassoon IHC	

Chapter 1: Introduction

1.1 Epidemiology of spinal cord injury (SCI)

Knowing the incidence and prevalence of SCI as well as its primary causes, is significant for guiding research, developing prevention strategies, and for health care planning. The incidence of SCI refers to the number of new SCI cases arising over a specified period of time and the prevalence refers to the number of individuals living with SCI over a specified period of time. In Canada, the incidence of SCI is ~2,000 new cases per year with a prevalence of ~86, 000 persons¹. In the United States, the incidence rate is ~17, 000 new cases per year with a prevalence of ~282, 000 persons². The leading cause of SCI varies worldwide and between age groups. In Canada, unintentional falls is the predominate cause of traumatic SCI in the elderly population whereas transport injuries and intentional injuries are more frequent in individuals less than 40 years of age³. The causes of traumatic SCI in the United States are similar to Canada but SCI due to acts of violence (e.g., gun shot wounds) are much more common². Following a SCI, nearly every aspect of a person's life – physical health, work, personal relationships, and recreation may be affected. The burden of a SCI is substantial and knowing the incidence and understanding the physiological mechanisms underlying a SCI can guide the development of prevention strategies, the development of treatments, and overall, improve the quality of life for those living with SCI.

1.2 Pathophysiology of SCI

Primary SCI is the immediate mechanical damage sustained to the spinal cord. Examples of a primary injury include compression of or lacerations to the spinal cord. The level at which the SCI occurs (e.g., cervical vs. lumbar) and the extent of damage (e.g., anatomically complete,

severing all neural connections across the lesion site(s) or anatomically incomplete, leaving spared ascending and descending connections) determines the amount of sensation and functional abilities that may be retained. The primary SCI does not only damage ascending and descending axon tracts; a SCI damages interneuron circuits in the spinal grey matter, supporting glial cells, blood vessels, cell membranes, and the blood brain barrier, among other factors. In doing so, the primary SCI initiates a cascade of biochemical and cellular events that sustains the initial damage to the spinal cord and spreads the damage to the spinal cord beyond the initial site of impact. This cascade of events is often referred to as secondary SCI⁴. Mechanisms of secondary SCI include excitotoxicity, ischemia and hypoxia to the spinal cord, and inflammation of the spinal cord⁵. The injury to axons in the spinal cord also triggers a process known as Wallerian degeneration⁶. Wallerian degeneration is the break down of myelin and axon distal to the site of injury (the portion of axon that becomes detached from the cell body) and this process is the first step to “repairing” central nervous system (CNS) damage.

In the CNS, injured axons are limited in their ability to regenerate and promote neurite outgrowth compared to axons injured in the peripheral nervous system (PNS). In the PNS, following Wallerian degeneration, the proximal portion of axons (attached to the cell body) are able to regenerate and reinnervate their targets due to the upregulation of regeneration associated factors (e.g., c-Jun⁷, activating transcription factor-3⁸, and growth associated protein-43 (GAP-43)⁹). The efficient removal of myelin (formed by Schwann cells) by macrophages in the PNS also contributes to axon regeneration as myelin contains molecules inhibitory to axonal growth including myelin-associated glycoproteins (MAGs)¹⁰. Conversely, in the CNS, the effects of upregulating regeneration associated factors following axon injury may be counteracted by the prolonged clearance of myelin^{9,11} (formed by oligodendrocytes) leading to limited regeneration

and neurite outgrowth in the CNS. Myelin was mostly cleared from the PNS around 30-days after an injury whereas myelin debris in the CNS was still prominent at 90-days after an injury¹¹. Oligodendrocytes contain myelin-associated inhibitory molecules including Nogo¹², myelin-associated glycoprotein (MAG)¹³, and oligodendrocyte myelin glycoprotein¹⁴. These molecules interact with the Nogo-66 receptor, activating a signalling pathway inhibitory to neurite outgrowth that starts with the ras homolog family member A (RhoA)¹⁴⁻¹⁷. Activated RhoA targets Rho-associated coiled-coil-containing protein kinase (ROCK), a downstream effector that regulates neuron cytoskeleton dynamics¹⁸. The isoform ROCK2 is primarily expressed in CNS tissue and its activity triggers LIM domain kinase (LIMK) leading to growth cone collapse^{19,20}. Interfering with RhoA or ROCK2 activity has been shown to promote axon regeneration after an injury^{21,22}.

Following a SCI, there is also the formation of a glial scar, a neuroprotective barrier that encloses the site of injury and limits the spread of SCI damage²³. Secondary damage cause astrocytes to become reactive and they crosslink to form the glial scar along with other CNS molecules such as microglia and oligodendrocyte precursor cells (OPCs)^{24,25}. Faulkner et al., 2004²⁶ demonstrated that glial scar formation in SCI mice can restrict CNS inflammation and cellular degeneration, protecting spared CNS tissue and improving functional outcomes after a SCI compared to mice without glial scar formation. However, the glial scar is considered a double-edged sword because it provides neuroprotection but also acts as a physical and biochemical barrier to neurite outgrowth across the injury site, and this is thought to limit functional recovery (Reviewed in Yang et al., 2020²⁷). Reactive astrocytes and OPCs express molecules called chondroitin sulfate proteoglycans (CSPGs), potent inhibitors of neurite outgrowth²⁸. CSPGs interact with the protein tyrosine phosphatase sigma receptor (PTP σ)²⁹, leukocyte common

antigen-related phosphatase receptor (LAR)³⁰, and Nogo receptor³¹ on neurons to trigger signalling cascades that inhibit neurite outgrowth. CSPGs are also found diffusely in the CNS extracellular matrix (reviewed in Galtrey et al.,2008³² and Avram et al.,2014³³) and concentrated within the ECM structure called the perineuronal network (PNN)³², further contributing to neurite outgrowth inhibition in the adult spinal cord. The PNN acts to stabilize the synaptic and intrinsic physiology of neurons³⁴. In addition to growth inhibitory molecules, adult neurons have a limited intrinsic capacity to support neurite outgrowth. Cyclic adenosine monophosphate (cAMP)³⁵ and mammalian target of rapamycin (mTOR)³⁶ are signalling pathways that modulate the intrinsic ability of neurons to promote neurite outgrowth. The activity of these signalling pathways are down-regulated in adulthood, contributing to the reduced ability of neurons to support neurite outgrowth^{35,36}. Collectively, there are a number of intrinsic and extrinsic factors that limit neurite outgrowth and spinal cord repair following an SCI.

1.3 The development of pharmacological treatments to improve recovery following an SCI

Plasticity promoting treatments can target various processes or structures in the CNS to promote functional outcomes following a SCI. These include increasing the intrinsic capacity of neurons to promote neurite outgrowth, restoring the integrity of neurons surrounding the SCI, or neutralizing growth inhibitory factors in the CNS environment.

mTOR and cAMP signaling pathways are upregulated in neurons during development to promote neurite outgrowth³⁵⁻³⁷. As development progresses, both pathways undergo an age associated decline, contributing to the reduced ability of neurons to support neurite outgrowth³⁵⁻³⁸. Following a SCI, mTOR^{36,37} and cAMP³⁹ signalling are further down regulated, limiting the capacity of adult neurons to induce neurite outgrowth and repair the spinal cord after injury. To

mitigate the decline in mTOR signalling, Liu et al., 2010³⁷ demonstrated that inhibiting phosphatase and tensin homolog (PTEN), an upstream negative regulator of mTOR, following an SCI maintained mTOR activity at a level similar to non-injured control mice. This led to neurite outgrowth from injured corticospinal tract (CST) neurons. Other studies have shown that administration of cAMP analogues or inhibitors of cAMP breakdown can restore cAMP levels after SCI and encourage neurite outgrowth^{40,41}. Therefore, increasing the activity of signalling pathways that encourage neurite outgrowth from neurons is one approach to repairing the injured spinal cord.

The break down of myelin in the CNS occurs during Wallerian degeneration however, Blight, 1985⁴² also noted that spared axons surrounding the lesion site became demyelinated around 7 days after SCI. The myelin sheath is important for rapid neural impulse propagation through a process called “saltatory conduction”. As such, disruption of axon myelination can slow and impair impulse conduction through an axon and consequently, impair motor and sensory function⁴³⁻⁴⁵. Demyelination may also leave axons more susceptible to axonal degeneration^{46,47}, further contributing to the limited recovery following an SCI⁴⁸. The goal of remyelination is therefore to restore impulse transmission through axons but also to protect and support the survival of axons⁴⁹. One method to promote remyelination is the transplantation of neural progenitor cells (NPCs) with robust potential to differentiate into oligodendrocytes. In studies conducted by Karimi-Abdolrezaee et al., 2006⁵⁰, NPC-derived oligodendrocytes were found to integrate primarily into the spinal white matter and ensheath axon tracts. The remyelination of axons was associated with improvements in the Basso, Beattie, and Bresnahan (BBB) open field assessment of locomotor function and the grid walking task in mice with a SCI⁵⁰. Another approach that has been widely explored is the neutralization of growth inhibitory molecules in

the CNS environment. Targeting Nogo-A is one option. Studies conducted by Simonen et al., 2003⁵¹ demonstrated that Nogo-A knockout mice had more neurite outgrowth around, caudal, and into the injury site from the CST compared to wildtype mice following a thoracic dorsal hemisection SCI⁵¹. Targeting the Nogo-66 receptor is another, potentially more effective option to neutralize growth inhibitor molecules in the CNS as oligodendrocyte-associated inhibitory molecules can all signal through the Nogo receptor. Studies conducted by GrandPre et al., 2002⁵² demonstrated that blocking the Nogo-66 receptor using a Nogo antagonist peptide enabled robust axon regeneration from the transected CST. CST fibers regenerated up to 15mm in length and the number of CST fibers caudal to the lesion was approximately 10% of the total CST fibers labelled rostral to the injury. Neutralizing the inhibitory effect of CSPGs is another widely explored treatment approach to SCI. Chondroitinase ABC (ChABC) is a bacterial enzyme that digests the chondroitin sulfate glycosaminoglycan side chains on CSPGs, inactivating their inhibitory effect. ChABC can be targeted to CSPGs in the glial scar or within the PNN in the spinal grey matter. Both approaches have been shown to increase neurite outgrowth following an SCI and translate into functional recovery. Bradbury et al., 2002⁵³ demonstrated that intrathecal administration of ChABC digested CSGPs at the SCI site and promoted the regeneration of sensory and CST axons following a C4 crush SCI. In primate models of SCI, Rosenzweig et al., 2019⁵⁴ demonstrated that ChABC targeted into the spinal grey mater significantly increased neurite outgrowth from the CST and translated into improved recovery of forelimb use in a food retrieval task. ChABC treatment has been developed over decades with significant advancements in delivery to the injured spinal cord ranging from gene therapy⁵⁵ to nano particles⁵⁶, each advancement showing more promise as an intervention to improve SCI outcomes⁵⁷.

While all of these approaches to improve functional outcomes after SCI have shown some results, there are numerous factors restricting neurite outgrowth and spinal cord repair after an injury. By targeting only one factor limiting neurite outgrowth, recovery following SCI is restricted.

1.4 Combinatorial pharmacological treatments

To target multiple factors that limit regeneration and neurite outgrowth following a SCI, the additive effects of combining more than one plasticity promoting treatment have been tested with the aim of increasing neurite outgrowth beyond the capabilities of treatments that target only one limiting factor. Treatments, including scar reducing agents, the upregulation of neurite outgrowth promoting pathways, the application of neurotrophic factors, and the implantation of cell grafts can be combined in different ways to bolster neurite outgrowth and functional recovery.

For example, Fouad et al., 2005⁵⁸ took ChABC treatment one step further and administered ChABC treatment rostral and caudal to the injury site in conjunction with implantation of Schwann cells (SC) and olfactory ensheathing glia (OEGs) in a complete thoracic transection model of SCI. The transection site was bridged using a gel containing SC, cells that surround peripheral nerves and express genes that support axon regeneration, providing a permissive substrate for axon regeneration across the injury site⁵⁸. OEGs, cells similar to SCs that enable the regeneration of axons in the olfactory system,⁵⁹ were placed rostral and caudal to the bridge to enable regenerated axons to exit the bridge and re-enter the spinal cord. ChABC served to digest growth inhibitory CSPGs, decreasing the growth inhibitory environment of the CNS. This combination treatment increased the number of myelinated axons and serotonergic fibers crossing the SC bridge into the caudal spinal cord⁵⁸. Axon growth across the injury site was

accompanied by functional improvements assessed using the BBB score and forelimb/hindlimb coupling⁵⁸. By combining more than one pharmacological treatment, multiple CNS factors can be targeted to encourage neurite outgrowth to encourage a greater plasticity after an injury.

1.5 Rehabilitative treatment following a SCI

The benefit of rehabilitative training is based on the observations of Hubel and Wiesel⁶⁰ in the visual cortex indicating that neurons and connections that are not used are lost and from Hebb's postulate⁶¹, the idea that connections between neurons are strengthened when they are simultaneously activated. Rehabilitative training can trigger coordinated neuronal activity that maintains and strengthens the neuronal connections being used to carry out tasks. This is true for both animal models of SCI and humans living with SCI. When neuronal connections are not used, the CNS reorganizes accordingly. For example, the region of the motor cortex representing and controlling hindlimb movements reorganized in rats with a bilateral transection of the CST in the thoracic spine⁶². Stimulation of the cortical region that previously only triggered only hindlimb movement in intact rats, triggered forelimb, whisker, and trunk activity in SCI rats⁶². Likewise, primates with amputation of forelimb or hindlimbs demonstrate motor cortex reorganization⁶³. Stimulation of deafferented regions in the motor cortex triggered activity of proximal muscle groups (e.g., the trunk) and adjacent body regions (e.g., the shoulder for forelimb amputation or the tail for hindlimb amputation)⁶³. Rehabilitative training not only maintains neuronal circuitry and strengthens connections, but it has been shown to encourage neurite outgrowth in the spinal cord, and this outgrowth is associated with improvements in functional recovery following an SCI. For example, rats with a C2/C3 SCI ipsilateral to their dominant paw showed improvements on the single pellet grasping (SPG) task after receiving

task specific training compared to untrained rats⁶⁴. This improvement was accompanied by an increase in sprouting of collateral fibers from injured and uninjured CST fibers rostral to the SCI⁶⁴.

However, it is important to note that structured rehabilitative training is not necessarily required to maintain neuronal circuitry or promote neurite outgrowth following an SCI. In Fouad et al., 2000⁶⁵, rats with a T8 dorsal transection injury receiving treadmill training daily for 5 weeks did not significantly improve in locomotor function compared to rats who did not receive rehabilitative training. It was thought that spared fibers in the ventral and ventro-lateral aspect of the spinal cord in untrained rats were able to sprout and compensate for the SCI because rats were not restricted in their daily activities and therefore able to 'self-train' (e.g., cage rearing and exploration). This aspect of self-training was able to promote spinal cord repair to such an extent that the addition of treadmill training did not provide significant functional improvement for trained rats⁶⁵. These results support a concept in SCI called spontaneous recovery whereby spared axons and spared neuronal circuits are capable of promoting some extent of functional recovery in the absence of training or interventions⁶⁶⁻⁶⁹. Rehabilitative training may be required in contexts where self-training is restricted.

The mechanisms by which rehabilitative training is thought to improve functional recovery are largely due to intrinsic changes within the neurons activated by the training. These mechanisms include the upregulation of neurotrophic factors such as brain-derived neurotrophic factor (BDNF)⁷⁰ or enhancing cAMP signalling in neurons⁷¹, which in turn, stimulate neurite outgrowth and changes in neuronal connectivity within the spinal cord. In a clinical setting, patients living with an SCI are encouraged to participate in rehabilitative training due to its strong association with improved functional recovery⁷². Due to the frequent use of rehabilitative training clinically,

researchers studying pharmacological treatments aimed at improving functional outcomes following an SCI should consider incorporating rehabilitative training into their experimental design.

Similar to rehabilitative training, electrical stimulation (ES) of muscles and nerves is another approach to promote recovery after SCI. ES provides low electrical impulses to nerves and muscles to help restore function and harnesses intact neural systems, spared by the SCI to promote functional recovery, not only of walking or moving but also restoring bladder function, respiratory function, or stimulating muscles to prevent pressure ulcers⁷³. The mechanism by which electrical stimulation promotes functional recovery is similar to that of rehabilitative training. Electrical stimulation triggers the activity of neuronal circuitry but can also activate neurite outgrowth promoting pathways to promote axonal sprouting and regeneration including the cAMP pathways⁷⁴ and BDNF expression⁷⁵. FES is increasingly used in clinical settings to encourage recovery after SCI⁷³.

1.6 Benefits of combining rehabilitative training with pharmacological treatments

A prominent combinatorial treatment in the literature is pairing of ChABC with rehabilitative training. ChABC treatment targets extrinsic inhibitors of neurite outgrowth while rehabilitative training boosts the ability of neurons to induce neurite outgrowth. In other words, ChABC treatment combined with rehabilitative training can amplify neurite outgrowth beyond what training alone can achieve by targeting more than one factor limiting neurite outgrowth after an SCI. Training, in turn, can not only induce neurite outgrowth but it can activate the newly formed neurite outgrowth and spared neuronal circuitry to rewire the injured spinal cord. For example, Garcias-Alias et al., 2009⁷⁶ demonstrated that rats with a cervical SCI receiving both

ChABC and rehabilitative training were able to regain the grasping technique used prior to the SCI. Rat receiving only rehabilitative training showed motor recovery; however, they had to rely on compensatory strategies (e.g., scooping pellets rather than grasping and lifting pellets) to retrieve pellets. The therapeutic potential of combining a pharmacological treatment with rehabilitative training is significant and should be further explored in the preclinical development of pharmacological treatments to enhance recovery following a SCI.

1.7 Emergence of a new pharmacological treatment to promote neurite outgrowth following an SCI

Recently, a new treatment avenue is being explored using an endogenously occurring growth factor called pleiotrophin (PTN). PTN (also known as HB-GAM) was first described by Rauvala, 1989⁷⁷ and later named PTN by another group of researchers⁷⁸. PTN is unique compared to other pharmacological treatments for SCI as it can simultaneously neutralize CSPGs while also amplifying the neurite outgrowth promoting pathways mediated by the glypican-2 receptor and the anaplastic lymphoma kinase (ALK receptor). These characteristics give PTN the additive therapeutic advantage of a combinatorial pharmacological treatments however, only one treatment needs to be administered following SCI.

PTN has a particularly important role in the development of the central nervous system (CNS) and a significant role in the neuroprotection and maintenance of neural circuits in adulthood^{79,80}. During development, PTN is secreted by neurons and glial cells to regulate the development of the CNS, specifically neurite outgrowth^{77,81}. It acts as an axon guidance cue in the formation of neural connections⁸². PTN expression peaks around 1-3 weeks postnatal and its expression declines into adulthood⁸³. In adults, PTN is associated with numerous physiological processes including metabolism, angiogenesis, inflammation, bone development, reproduction, and cancer

(reviewed in Wang, 2020⁸⁴). PTN expression in the adult CNS is limited to select neuron populations including the hippocampal CA1-3 regions and the cerebral cortex laminae II-IV⁸⁵. It is also secreted by pericytes (support cells found on capillaries in the CNS)⁸⁶. Studies by Krellman et al., 2014⁷⁹ showed that PTN knock-out mice had significant abnormalities in their behaviour and cognitive function, and this was caused by changes in neural density in the entorhinal cortex, a region of the brain important for learning and memory. These studies demonstrate the importance of PTN expression to both the development and maintenance of the CNS.

PTN expression in the CNS is endogenously upregulated in response to various physiological processes. In the context of neuropathologies, there is evidence that PTN modulates neuronal changes in the nucleus accumbens, a brain structure primarily involved in reward circuitry, following amphetamine use⁸⁷. PTN is also secreted by tumour-associated macrophages in glioblastomas leading to tumour growth⁸⁸. In the context of CNS injury, upregulation of PTN expression is associated with restorative effects to the CNS. Rats with ischemic brain injuries showed increased PTN gene transcription and protein expression in microglia and macrophages⁸⁹. The elevated levels of PTN contributed to the recovery in rats by stimulating neovascularization⁸⁹. Following a traumatic SCI, endogenous PTN expression increased in both surviving neurons and glial cells surrounding the injury site and was thought to contribute to the recovery process by stimulating regeneration and synaptogenesis⁹⁰. These studies demonstrate that PTN is a versatile growth factor and that high levels of PTN expression can lead to negative consequences or have beneficial effects depending on the context in which it is upregulated.

The discovery that PTN upregulation occurs endogenously to contribute to CNS repair after an injury has been of particular interest to researchers developing treatments to repair the CNS and

promote functional recovery after an injury. Researchers have examined the outcome(s) of artificially upregulating PTN following a CNS injury and whether this upregulation benefits recovery both anatomically (e.g., neurite outgrowth) and functionally (e.g., motor and/or sensory function). In a study by Paveliev et al., 2016⁹¹, PTN treatment following a prick injury to the cerebral cortex (made by inserting a 30G needle into the cerebral cortex) resulted in the regeneration of dendrites. In mice with a transection SCI, PTN administered into the injury site at the time of SCI, increased the number of sensory axons that approached and or crossed the injury site⁹¹. Additionally, these axons were higher in complexity and number of branch points coinciding with findings from Fenrich et al., 2011 that highly branched axons terminals are more successful at regenerating across transection SCI. More recently, PTN injected into the SCI site and administered intrathecally into mice with a lateral hemicontusion injury has been linked to motor improvements in mice models of SCI⁹².

There are 2 major receptors through which PTN is thought to contribute to the regeneration of injured axons and neurite outgrowth from axons surrounding the injury site. The first is the ALK receptor^{93,94} and the second is the glypican-2 receptor⁹¹. Both receptors are highly expressed on CNS neurons and both receptors trigger signalling cascades that encourage neurite outgrowth. Given the versatility of PTN, it is highly likely that PTN interacts with both receptors in some capacity to encourage neurite outgrowth. What is notable about the glypican-2 receptor pathway is that PTN interacts with the glypican-2 receptor as a complex with CSPGs⁹¹. By binding to CSPGs, not only does PTN trigger a neurite outgrowth promoting pathway, PTN effectively inactivates the inhibitory effect of CSPGs. CSPGs are present throughout the CNS extracellular matrix, concentrated within PNNs and upregulated following an SCI in the glial scar and rostral-caudal to the site of SCI (see section 1.2, Pathophysiology of SCI). The mechanism of PTN is

most similar to ChABC in that ChABC inactivates CSPGs to eliminate their growth inhibitory effect. There is strong evidence in the literature supporting the therapeutic potential of ChABC to increase neurite outgrowth following a CNS injury and promotes significant functional recovery^{53,54,76,95}. However, it is unclear whether ChABC is capable of activating neurite outgrowth promoting pathways. The interaction of PTN with glypican-2, therefore, gives PTN a unique dual mechanism to promote neurite outgrowth that, in theory, could transcend the therapeutic potential of ChABC. Furthermore, ChABC is not an endogenously occurring enzyme, it is isolated from *Proteus Vulgaris* and the stability of ChABC activity in the CNS has been reported differently by researchers. Tester et al., 2007⁹⁶ showed that the enzymatic activity of ChABC rapidly degrades at body temperature (37°C) after three days and at 39°C, ChABC is degraded within 1 day⁹⁶. They also examined 9 different lots of ChABC and found that ChABC activity varied between lots, lasting 1 day at the minimum and 6 days at the maximum⁹⁶.

PTN has been studied for several decades but it was only more recently that researchers started to administer exogenous PTN into *in vivo* models of CNS injury and examine the effects on recovery. What my thesis aimed to do was to further understand the capabilities of PTN to promote neurite outgrowth *in vivo* and in doing so, develop PTN as a potential treatment to encourage functional recovery following an SCI. We studied rat models of SCI treated with PTN targeted into the spinal cord rostral and caudal to the SCI site. Neurite outgrowth rostral and caudal to the injury site has been strongly linked to functional recovery following SCI. Spared axons and neurons denervated by the SCI can sprout and form new connections to bypass the SCI site and in essence, rewire the spinal cord^{62,97-103}. PTN treatment targeted to different locations surrounding the SCI site may have effects on neurite outgrowth. Spared axons

surrounding the lesion site and neurons denervated by the SCI may respond differently to PTN treatment, potentially leading to differences in functional outcomes.

To assess for changes in functional outcomes resulting from PTN treatment after SCI, we used the SPG task. The SPG task requires fine motor function of the distal forelimb controlled by the CST and rubrospinal tract (RST) in the spinal cord. As such, the SCI models used in all experiments intended to injure the CST and RST unilaterally to impair forelimb motor function of the unilateral forepaw. Sprouting was measured only from the CST however, as this tract originates from the motor cortex which can be more reliably traced than the RST which originates from the red nucleus in the ventral midbrain.

There were three aims to my thesis:

- 1) to determine the dose of PTN to maximize neurite outgrowth following SCI,
- 2) to determine the location(s) of PTN administration (e.g., rostral or caudal of an SCI) that would encourage the most functional recovery, and
- 3) to determine if there is a complementary effect to combining PTN treatment with rehabilitative training using the single pellet reaching and grasping (SPG) task.

Several experiments were designed to assess these aims. For clarity, the title of each experiment included in my thesis is listed here, along with a summary of the purpose of the experiment in relation to the aims presented.

- *PTN in vitro using cortical cell cultures*
- *PTN dose-response examining neurite outgrowth*

- *PTN vs. ChABC in vivo*
- *PTN following a contusion SCI*
- *PTN DLQ SCI*

The *PTN in vitro* experiment was to ensure our supply of PTN promoted neurite outgrowth at a level similar to what has been reported in the literature. The *PTN vs. ChABC* experiment was also intended to ensure PTN could promote neurite outgrowth but in an *in vivo* model of SCI. Neurite outgrowth from PTN was compared to ChABC in this experiment to screen for any potential differences in neurite outgrowth between treatments. The *PTN dose-response* experiment intended to address aim 1 and thereby, apply an optimal dose of PTN in subsequent experiments. PTN has been administered in previous *in vivo* studies⁹¹ at a concentration of 1.0 mg/mL however, the rationale for this concentration has yet to be provided. Male and female rats were used in this experiment to examine for sex differences in neurite outgrowth. The *PTN contusion SCI* and *PTN DLQ SCI* experiments were carried out to address aims 2 and 3. In the PTN contusion SCI experiment, PTN was targeted bilaterally rostral and caudal to the SCI however, in the PTN DLQ SCI experiment, PTN was only target caudal and ipsilesional to the SCI to determine if treatment location affects neurite outgrowth and functional recovery. A contusion model of SCI was used initially, however, adjustments to the experimental design were made based on the experimental results obtained leading us to switch to a DLQ model of SCI in the subsequent experiment (full details are provided in the methods and results sections). The SPG task was used for rehabilitative training as a measure of functional recovery following SCI and PTN treatment.

Chapter 2: Methods

2.1 Animal care and ethics:

All experimental procedures were approved by the Health Sciences Animal Care and Use Committee of the University of Alberta. Lewis rats from Charles River Laboratories Canada were used for all experiments and arrived weighing between 180-220 g. Rats were housed 2 per cage with a 12-hour light/dark cycle. Water and food were provided *ad libitum* except during the single pellet grasping (SPG) training when rats were trained 5 days per week and food restricted to 90% of their normal daily intake on the days before completing the task. This was done to motivate their participation in SPG training. The number of rats used for each experiment varied based on the purpose of the study.

- *PTN dose-response*: N=40 (20 males and 20 females), n=8 per experimental group (4 males, 4 females)
- *PTN vs. ChABC*: N=9 (females), n=3 per experimental group
- *PTN Contusion SCI*: N= 24 (females), n=12 per experimental group
- *PTN DLQ SCI*: N=24 (females), n=12 per experimental group

2.2 PTN and ChABC preparation:

Preparation of PTN

PTN was obtained on two occasions from the laboratory of Dr. H. Rauvala. The first batch of PTN arrived as a 1 mL aliquot at a concentration of 2 mg/mL and the second batch of PTN arrived as a 1.1 mL aliquot at a concentration of 5 mg/mL. PTN was suspended in 1 M NaCl in a 20 mM phosphate buffer upon arrival. To exchange the buffer for PBS, 4 mL of PBS was added to the samples and centrifuged using Amicon-Ultra 4 (Millipore, UFC800308) at 6000 for

approximately 40 minutes until the original volume of the sample was reached. The Amicon-Ultra 4 filter has a molecular weight cut-off of 3 kDa, allowing only molecules smaller than 3 kDa to pass, therefore, PTN protein should not have been lost during centrifugation and buffer exchange. The sample was then sterilized using a Spin-X centrifuge tube (Costar, 8160) at 10,000 for 2 minutes. After exchanging the buffer, PTN was diluted to the required concentrations by adding specific volumes of PBS to achieve the desired concentration. To concentrate PTN to higher concentrations, PTN aliquots were centrifuged using Pierce Protein Concentrator filter tubes with a molecular weight cut-off of 3 kDa (Thermo Scientific, 88512) designed to allow buffers to pass through the filter but not PTN. The concentrations of PTN were tested using a DC protein assay (Thermo scientific, 23227) before being used for any experiment according to the protocol provided by the kit. For this protocol, 8 standards were made using bovine serum albumin in sterile PBS to generate a line of best fit to which the sample of unknown concentration of PTN could be interpolated. Standards were made by serially diluting BSA at 25 mg/mL to a final concentration of 0.195 mg/mL. These standards were then loaded into the wells on a flat-bottom 96-well plate in 5 μ L aliquots alongside aliquots of the sample of unknown concentration of PTN. After, 5 μ L of 'Reagent A' (alkaline medium) and 200 μ L of 'Reagent B' (copper (Cu^{2+}) salt solution) was added to each well to react with the protein in each well and induce a colour change that can be analyzed by a spectrophotometer. The intensity of the colour change is proportional to the concentration of protein in the sample. The reagents within each well were mixed thoroughly using a plate shaker for 30 seconds. The plate was covered using the well plate lid and incubated at 37 $^{\circ}\text{C}$ for 30 minutes. The plate was then read on a Biorad xMark™ microplate spectrophotometer (Bio-Rad Laboratories, 168-1150) at A280 nm. The spectrophotometer emits light at a wavelength of 280 nm at the sample within the wells

and measures the amount of light that passes through. There is an inverse relationship between the amount of light that passes through the sample and the concentration of protein within the sample. The light measurements are processed using the Microplate Manager software (Bio-Rad Laboratories, 168-9520) to provide a read-out of the protein concentration in each well.

Preparation of ChABC

Five units of ChABC were ordered from Sigma-Aldrich, C3667. ChABC was prepared according to the protocol provided by the suppliers to make a solution of ChABC at a concentration of 1.33 U/ μ l (0.1 U of ChABC per 0.75 μ l volume injection). This concentration of ChABC was consistent with other studies administering PTN into the spinal cord rostral and caudal to the SCI^{104,105}.

2.3 Cortical cell cultures:

This protocol was taken from the laboratory of Dr. I. Winship. Cell cultures and epifluorescent imaging for the *PTN in vitro* experiment was carried out by a graduate student, Somnath Gupta. The protocol used in my experiments was similar to the protocol used for the cell cultures and for epifluorescent imaging published in Gupta et al., 2021⁹⁴. Mr. S. Gupta provided epifluorescent images of the cell cultures and I carried out the analysis of neurite extension using the NeurphologyJ extension on ImageJ.

Matrices preparation:

Glass coverslips were treated with 100 μ g/mL 1-poly-L-Lysine (Sigma-Aldrich, P5899, USA) for 2 hours. Coverslips were washed 3x with water and then coated with either a growth permissive (10 μ g/mL of laminin (Corning, 354232)) or growth inhibitory matrix (10 μ g/mL of laminin +

1.25 $\mu\text{g}/\text{mL}$ CSPGs or 10 $\mu\text{g}/\text{mL}$ of laminin + 10 $\mu\text{g}/\text{mL}$ CSPGs (Sigma-Aldrich, CC117) for 2 hours and then washed 2x with PBS.

Primary cortical neuron culture:

Rat primary cortical neurons were isolated from 0-1-day old Sprague Dawley rat pups. The brains were dissected from the pups and the cerebral cortices were separated from the dura as well as the midbrain and hindbrain structures. Cortices were then digested with TrypLE (Gibco, 12605-028) at 37 °C for 15-minutes. Cortical cells were isolated from the tissue by trituration in neurobasal A medium (Thermofisher, 1088802) which contained B27 supplement (1:50 v/v) (Gibco, 17504-044), antibiotics, and GlutamX (Gibco, 35050-061). On the prepared coverslips, 20,000 cells were seeded per well on a 24-well plate and treated with PTN (10 $\mu\text{g}/\text{mL}$) and then incubated at 37 °C, 5% CO₂.

Analysis of neurite extension:

Cortical cells were fixed after 72 hours of treatment with a 5% formaldehyde solution for 15 minutes. Cells were stained with microtubule-associated protein 2 antibody (MAP2, 1:500, Sigma Aldrich M9942, to visualize neurons), and imaged using epifluorescent microscopy. Analysis of neurite extension was done using the NeurphologyJ extension on ImageJ. Images of the well plates were uploaded onto ImageJ. Neurites were traced using the ‘pencil tool’ at a width of 2 pixels and soma with a width of 10 pixels. Traced images were then converted into 16-bit images for processing on the NeurphologyJ extension. The extension guides the user through each step. In general, thresholding of the image is done to isolate the neurites and soma. Any debris or excess pixels are removed using the ‘particle remover’ function. A summary file is

generated providing the number of soma in the image and the total neurite length of all neurites in the image. The total neurite length is divided by the total number of soma to obtain the average neurite length. Data is then compared between groups.

2.3 Surgical timing, preparation, and care:

The timing of SCI surgeries for each experiment was based on purpose of the experiment. For the *PTN dose response experiment and the PTN vs. ChABC experiment*, the experiments focused on neurite outgrowth changes therefore, no SPG rehabilitative training occurred. Some sensory and motor testing was performed (e.g., von Frey hair and horizontal ladder, respectively) however, only a baseline assessment was obtained prior to completing the SCI surgeries. The *PTN DLQ SCI experiment and PTN Contusion SCI experiment* examined the additive effects of PTN treatment with rehabilitative training. Therefore, SCI surgeries and spinal injections were not scheduled until the success rate of rats in the SPG task plateaued (reaching a state of little to no change in success rate for 2 or more weeks). Details regarding SPG training, von Frey hair testing, and horizontal ladder task can be found in the behavioural testing and rehabilitative training sections of the methods (2.7-2.8).

All surgeries were performed under isoflurane anesthesia. Rats were induced using 5% isoflurane (Sigma-Aldrich, 792632) in carbogen (5% CO₂, 95% O₂). During induction, the skin on the dorsal neck of the rats was shaved, and rats were placed into a stereotaxic frame to stabilize the head and cervical spine during surgery. After placement into the stereotaxic frame, rats were maintained on isoflurane at 2.5-3% in carbogen. At the onset of surgery, the shaved skin on the dorsal neck of the rats was disinfected with 10% chlorhexidine digluconate (Sigma-

Aldrich, PHR1294) and ethanol. Eyes were lubricated (Alcon Systane Ointment) to prevent corneal dehydration throughout the surgery. A heating mat set to 37 °C was used to prevent anesthesia-induced hypothermia. Following every surgery (regardless of the number of procedures), before recovery from anesthesia, all rats received 3 mL of saline and buprenorphine (0.3 mg/kg) for hydration and pain control, respectively. Rats were then placed into heated recovery cages with *ad libitum* food and water and the floor of these cages were lined with paper towel to absorb urine and moisture within the cage. Rats were returned into their home cage approximately 12-18 hours after their surgery, once their score on the grimace scale¹⁰⁶ was “moderately present” or “not present” and rats were actively exploring their recovery cages.

2.4 SCI surgeries:

Our rat models of SCI were created by damaging the spinal cord directly (rather than inflicting damage to the spinal cord through skin, muscle, and bone as would typically occur in a human SCI) and therefore, required the spinal cord to be exposed. To do so, the skin above the cervical level 2-5 (C2-C5) vertebrae was incised using a scalpel blade No.10 and the muscle above these vertebrae were spread apart using curved Metzenbaums to expose the C2-C5 vertebral bone. A unilateral laminectomy was performed at either the C4 or C5 level, depending on the SCI model used (SCI models are described in relation to each experiment below). Following the SCI surgery, muscles were sutured together with absorbable sutures, and the skin was closed using 9mm stainless steel clips.

PTN dose-response (Figure 1A): All rats received a right-side unilateral dorsal-lateral quadrant (DLQ) transection SCI at the cervical level 4 (C4)^{107,108}. No rehabilitative training occurred for these rats; therefore, the preferred paw of the rats was not determined. This injury is made by

inserting a thin blade at the midline on the dorsal side of the spinal cord to a depth of ~1 mm and sliding the blade laterally to the lesion approximately one-quarter (one quadrant) of the spinal cord. This injury model intends to injure the corticospinal tract (CST) and part of the rubrospinal tract (RST) ipsilateral to the side of SCI, tracts that are important for fine motor control of the distal forelimb.

PTN vs. ChABC (Figure 1B): All rats received a right unilateral DLQ transection injury at the C4 level. No rehabilitative training occurred for these rats; therefore, the preferred paw of the rats was not determined.

PTN contusion SCI (Figure 1C): All rats received a lateral hemi-contusion injury at cervical level 5 (C5) using an Infinite Horizon impactor (Precision Systems & Instrumentation, LLC) set to a force of 125 kdyns¹⁰⁹. Rats were placed into the impactor at an angle of 15° on the rostral-caudal axis using a customized frame to induce a lateral hemi-contusion 1.25 mm from the midline on the side of the rat's preferred paw determined during SPG training. This injury model causes a bruising injury to the spinal cord and intends to injure the CST and RST ipsilateral to the SCI to impair motor control of the distal forelimb.

PTN DLQ SCI (Figure 1D): All rats received a DLQ transection injury at the C4 level on the side of the rat's preferred paw determined during SPG training.

2.5 PTN spinal injection surgeries:

To be able to administer spinal injections rostral and caudal to the SCI, a partial laminectomy of the vertebrae unilateral to and above and below the level of the SCI was performed to expose more surface area of the spinal cord. If injections were provided only caudal to the SCI (e.g., the *PTN vs. ChABC experiment and the PTN DLQ SCI experiment*), a unilateral partial laminectomy

was only performed caudal and ipsilateral to the SCI. For the *PTN dose-response*, *PTN vs. ChABC*, and *PTN contusion SCI* experiments, spinal injections occurred at the time of SCI, therefore the partial laminectomy was performed when exposing the spinal cord for the SCI. For the *PTN DLQ SCI experiment*, spinal injections were given 13-days after the SCI and therefore, the spinal cord needed to be re-exposed according to the methods described in section 2.4 SCI Surgeries.

Spinal injections

Hamilton syringes (10 μ L) fitted with a glass capillary (1 mm outer diameter) pulled into a needle of <1 μ m in diameter were used to provide spinal injections in the *PTN dose-response* experiment. For the *PTN vs. ChABC*, *PTN contusion SCI*, and *PTN DLQ SCI experiments*, a 10 μ L blunt Hamilton syringe with a 34-gauge metal needle was used. The metal needles improved the accuracy of spinal injections because they were more stiff compared to glass capillaries and did not bend upon contacting the spinal cord. For all spinal injections, a 27-gauge needle was used to puncture the spinal dura to reduce the resistance against the spinal injection needle when providing the spinal injection. Spinal injections occurred over a 1- minute duration and the capillary or needle was left in the spinal cord for 1-minute following the injection to limit the backflow of PTN out of the injection site.

PTN dose-response (Figure 1A): Forty rats were randomly divided into 1 of 5 experimental groups: PBS (CTRL) or PTN at concentrations of either 0.5 mg/mL, 1.5mg/ml, 5 mg/mL, or 15 mg/mL. Spinal injections were made under the same anesthesia as the SCI surgery. Injections were made directly into the intermediate grey matter 0.75 mm lateral of the midline and 1.5 mm deep from the dorsal surface of the spinal cord. Three injections of 1 μ L were made into the SC

at the following locations: ~1 mm rostral to the lesion, ~1 mm rostral and contralateral to the lesion, and ~1 mm caudal to the lesion.

ChABC vs. PTN (Figure 1B): Nine rats were randomly divided into 3 experimental groups: PBS (CTRL), PTN, or ChABC. Spinal injections were made under the same anesthesia as the SCI surgery and injections were made directly into the intermediate grey matter 0.75 mm lateral of the midline and 1.5 mm deep from the dorsal surface of the spinal cord. Rats in the PTN group were injected with 0.75 μg of PTN (0.75 μl at 1.0mg/ml) 2-2.5 mm caudal and ipsilateral to the SCI. Rats in the ChABC group were injected with 0.1 U of ChABC (0.75 μl at 1.33 U/ μl).

PTN contusion SCI (Figure 1C): Twenty-four rats were randomly divided into 2 groups: PBS (CTRL) or PTN. Spinal injections were made under the same anesthesia as the SCI surgery and injections were made directly into the intermediate grey matter 0.75 mm lateral of the midline and 1.5 mm deep from the dorsal surface of the spinal cord. Injections were made into the spinal cord bilaterally ~2.5 mm rostral and ~2.5 mm caudal to the SCI (4 injections total). PTN was given at a concentration of 1.25 mg/mL. Injections were initially given at a volume of 1 μL (1.25 μg of PTN) on the first day of surgeries, however, rats were slow to recover after receiving 4 spinal injections at 1 μL and a contusion SCI. The volume of injections was therefore reduced to 0.75 μL (0.94 μg of PTN) on the second day of surgeries. An equal number of rats in the PTN treated and PBS treated groups received 1 μL and 0.75 μL injection volumes.

PTN DLQ SCI (Figure 1D): Twenty-four rats were randomly divided into 2 groups: PBS (CTRL) or PTN treated. It is important to note that spinal injections for this experiment occurred 13-days following the SCI surgery. This was done in response to the slow recovery of rats in the *PTN contusion SCI experiment* but also has the added benefit of being a more clinically relevant approach as SCI treatments are typically not administered at the time of SCI in humans. One

injection was made directly into the intermediate grey matter 0.75 mm lateral of the midline and 1.5 mm deep from the dorsal surface of the spinal cord. For these injections, a solution of 30% biotinylated dextran amine (BDA) (Invitrogen, BDA-10000, D1956) was added to a 10 μ L aliquot of PTN or PBS. PTN was co-injected with BDA so that the location of the spinal injection could be identified with more precision during histological analysis. Rats in the PTN group were injected with 0.9 μ g of PTN (0.75 μ L at 1.2 mg/mL).

2.6 AAV9 CST tracer injection surgeries:

The CST was traced by injecting an adeno-associated viruses serotype 9 (AAV9) containing a transgene to express tdTomato (AAV9-tdTom; Boyden Viruses, UNC Vector Core, NC, USA) or green fluorescent protein (AAV9-GFP; Boyden Viruses, UNC Vector Core, NC, USA) into the forelimb motor cortex . Tracing the CST allows CST fibres and any potential neurite outgrowth emerging from the CST to be visualized under fluorescent microscopy. The coordinates used to landmark the cortical injections were 1.5 mm lateral, 1.5mm rostral to Bregma, and 1.5mm deep¹¹⁰. Two 0.75 μ L injections of AAV9-tdTom (5.9×10^{12} vg/mL) were used and 3 x 0.75 μ L injections of AAV9-GFP (2.0×10^{12} vg/mL).

PTN dose-response (Figure 1A): AAV9-tdTom injections were made into the left forelimb motor cortex (contralesional) and AAV9-GFP injections were made into the right forelimb motor cortex (ipsilesional). This tracer surgery occurred under the same anesthesia as the SCI surgery. Cortical injections were made using Hamilton syringes (10 μ L) fitted with a glass capillary pulled into a needle of <1 μ m in diameter.

ChABC vs. PTN, PTN contusion SCI and PTN DLQ SCI (Figure 1B-D): Three changes were made to the AAV9 tracer surgeries after the PTN dose-response experiment: 1) AAV9-tdTom

injection volumes were reduced to 0.6 μ L to reduce the number of traced axons, 2) AAV9-tdTom was given in the ipsilesional forelimb motor cortex and AAV9-GFP into the contralesional forelimb motor cortex, and 3) cortical injections were made using a 10 μ L Hamilton syringe with a custom 32-gauge bevelled metal needle. The volume of tdTom injected was reduced because excess AAV9 tracing can limit the ability to distinguish between individual axons during CST fiber analysis and the intensity of the tracer at 2x 0.75 μ L overwhelmed the Leica HyD hybrid detector system during image acquisition in the *PTN dose-response*. The side of AAV9-GFP and tdTom injections were switched because tdTom is a more potent tracer than GFP, therefore, we wanted to increase the probability that contralesional CST fibers innervating the ipsilesional side could be detected during histological analysis. Lastly, custom metal needles were designed to improve the accuracy of cortical injections compared to needles made from glass capillaries.

2.7 Behavioural testing:

Horizontal ladder assessment

The horizontal ladder task¹¹¹ was used to assess functional recovery following an SCI and PTN treatment. The horizontal ladder apparatus had 1m long plexiglass walls with a thickness of 2 cm and height of 20 cm. The metal ladder rungs were 3mm in diameter and randomly spaced with distances ranging from 1-3cm. Rats were first acclimated to the ladder apparatus by allowing them to walk across the ladder 3 times on the day before the video recording. This acclimation phase was only done before recording the baseline videos (that is, before the SCI to assess the normal motor function of each rat). During the recorded assessments (60 fps, Panasonic, DMC-FZ200 camera; Full HD), each rat crossed the ladder 6 times, 3 times with the right paw facing the camera and 3 times with the left paw facing the camera. A mirror angled at 45° was placed

below the ladder and was included in the video recording to improve the visualization of each paw placement. The videos were analyzed to count the number of correct paw placements, slips, and misses. The percentage of missteps was then calculated by taking the sum of slips and misses made over the three crossings and dividing this number by the total number of steps taken over the three crossings. The average score within a group was taken and compared between groups to determine if there were any significant differences in motor recovery.

Von Frey hair assessment

An automated von Frey hair system (IITC Life Science, CA, USA) was used to assess the forepaw of rats for hyperalgesia and allodynia following PTN treatment. This system involves placing rats into plexiglass enclosures with metal grid floors. Rats were first acclimated to the enclosures by placing them in the enclosures for 10-minutes without any stimulation the day before testing. To carry out von Frey hair testing, the right and left forepaws of each rat were poked with the point of a rigid tip 5 times. The force required to elicit a sensory response (e.g., a paw raise or a paw lick) was recorded. The 3 recordings yielding the smallest standard deviation between the 5 trials were averaged and used as the score.

Timeline of horizontal ladder and Von Frey hair assessment

PTN dose-response: Rats were assessed for their baseline performance on the horizontal ladder (pre-SCI), and then at one, three, and 5-weeks post-SCI. For the von Frey analysis, rats were assessed for their baseline sensory response (pre-SCI), and then at 1-, 3-, 5-, and 7-weeks post-SCI.

PTN contusion SCI: Rats were assessed for their baseline performance on the horizontal ladder after their pre-SCI SPG success scores plateaued. Rats were then assessed at 2-weeks post-SCI to assess the severity of their injuries and a final time when their post-SCI SPG success scores plateaued. For the von Frey analysis, rats were assessed for their baseline sensory response after their pre-SCI SPG success scores plateaued. Rats were assessed post-SCI once their SPG success scores plateaued.

PTN DLQ SCI: Rats were assessed for their baseline performance after their SPG success scores plateaued. Rats had a final assessment once their post-SCI SPG success scores plateaued. For the von Frey analysis, rats were assessed for their baseline sensory response after their pre-SCI SPG success scores plateaued. Rats were assessed post-SCI once their SPG success scores plateaued.

2.8 Rehabilitative Training

SPG task

The SPG task was used to provide forelimb rehabilitative training to rats post-SCI. The task was carried out as described by Torres-Espín et al., 2018¹¹². For this task, rats were placed into a plexiglass enclosure with a slit on the front and back walls that allow access to a food pellet dispenser. The enclosure had metal grid floors which allow any dropped pellets to fall beyond the grasp of the rat. During pre-SCI training, rats learned to reach their paw through the slit and grasp a pellet presented on a pedestal (chocolate flavoured food pellet (Dustless Precision Pellets, Bio-Serv, NJ, USA) or sucrose pellet (TestDiet, 5TUT sucrose tab, St. Louis USA) in a 4:1 mix, respectively, to motivate their participation in the task). After 1 grasping attempt was made on one side of the enclosure, the had to walk rat and attempt a grasp on the other end of the enclosure. One week was required for rats to learn the task and to establish the rat's preferred

paw for the task. Rats were then trained 5-days per week for 10-minutes each day. Rats were filmed 1-day per week (60 fps, Panasonic, DMC-FZ200 camera; Full HD) by the researcher training the rats and the training videos were analyzed by a different laboratory member to blind the trainer to any treatment or experimental effects. Videos were analyzed to determine the number of times the animals dropped, knocked, or successfully grasped and retrieved a pellet. The success rate was calculated by dividing the number of successful retrievals by the total number of attempts made during the 10-minute session. Once the success rate of all rats' plateaued (~6 weeks), rats received their SCI surgery. Following the SCI surgery, rats were given 1 week to recover from the surgery, after which, they resumed SPG training. Post-SCI training occurred exactly as pre-SCI training; however, food restriction was not applied until rats recovered the weight lost from the SCI surgery. Post-SCI SPG training occurred until the success rate of all rats plateaued. SPG training was used in both the *PTN contusion SCI* experiment and the *PTN DLQ SCI* experiment.

High-speed SPG analysis

A detailed analysis of the reaching and grasping technique of each rat was analyzed as previously described in Whishaw et al., 2008 and Torres-Espin et al., 2018^{107,113}. High-speed video analyses were conducted once at baseline and once after the post-SCI SPG score plateau was noted (as this indicates the maximum performance rats achieve in the SPG task post-injury). For this analysis, rats were placed in a training enclosure and 3 successful reaching attempts were recorded at high-speed (120 fps, Panasonic DMC-FZ200; resolution of 1280 × 720 pixels). Each successful attempt was scored on 11 components as outlined in Whishaw et al., 2008. A score of 0 indicates that the movement is absent, 0.5 indicates the movement is present but

abnormal, and 1 indicates the movement is normal. The score is then averaged for each rat and the average scores per group are compared.

2.9 Histological analysis:

At the end point of each experiment, rats were euthanized using a lethal dose of Sodium Pentobarbital (100 mg/kg, 0.8 mL/200g, i.p.) and transcardially perfused with saline followed by a 0.1 M PB solution containing 4% formalin and 5% sucrose. The spinal cord and brain of each rat was extracted and post-fixed in the same formalin-sucrose solution for 2-hours. The tissues were then transferred into a 0.1 M PB solution containing 30% sucrose for 5-days for cryoprotection.

The spinal tissue was prepared for sectioning by embedding a 1 cm block of tissue, ~5cm above and below the SCI, in O.C.T. (Sakura Finetek, USA). A 1 cm block ensured all injection sites were included in the same tissue block as the SCI. Sectioning of each block of tissue would therefore depict the progression of spinal tissue from rostral injection to SCI to caudal spinal injection. The block of spinal tissue was then mounted onto filter paper, frozen in 2-methyl butane at -60 °C (dry ice), and stored at -80°C until sectioned.

Using a NX70 cryostat (Fisher Scientific), spinal cords were cut coronally at a thickness of 35µm in the *PTN dose-response* experiment and a thickness of 25µm in the *ChABC vs. PTN*, *PTN contusion SCI* and *PTN DLQ SCI* experiments. A thickness of 35µm was used in the dose response experiment to increase the efficiency of spinal sectioning for 40 rats. A thickness of 25 µm was used in subsequent experiments when the number of rats per group was lower.

Sectioning was done in series, over 8 slides such that each slide gave a representation of the entire tissue block. For the *PTN dose-response* experiment, only every other section of tissue was kept and mounted onto the slide, again, to increase the efficiency of tissue sectioning in this experiment. Tissue slides were stored at -20 °C until further processing.

Lesion analysis

For all experiments, a 0.5% cresyl violet solution was used to stain 1 slide of tissue per rat. This slide was then visualized under light field and phase-contrast microscopy (Leica DM6000B, camera Leica DFC350 FX) using a 10x objective lens to observe the lesioned area. The tissue cross-section showing the largest area of SCI damage was imaged and considered the lesion epicentre. The total lesioned area was measured using ImageJ software and calculated as a percentage of the total area of the spinal cord cross-section. The spinal injection sites were also counterstained with the cresyl violet stain and were visualized using light microscopy. The imaged spinal section(s) over which the injection sites could be identified were recorded to guide the neurite outgrowth analysis (see below).

2.10 Immunohistochemistry:

3,3'-diaminobenzidine (DAB) stain

DAB staining was used to visualize the BDA that was co-injected with PTN in the *PTN DLQ SCI* experiment to more accurately pinpoint the site of the spinal injection. One slide of tissue per rat was dehydrated at 37°C for 1hr, rehydrated in TBS (0.5%) for 10-minutes x2, and then incubated in TBS-Tx for 2x 45-minutes. Slides were then incubated overnight at 4°C in the Vectastain ABC reagent (Vectastain ABC Kit, Vector Laboratories, PK6100) prepared according

to the instructions provided by the manufacturer. Slides were washed 2 x 10 min in TBS to remove unbound ABC. The DAB reagent (Vector DAB kit, Vector Laboratories, SK4100, prepared according to manufacturer instructions) was then applied to the tissue and remained on the tissue for ~30-seconds until the reagent reacted sufficiently with the BDA (i.e., the tissue changed from colorless translucent to light brown). The reaction was then neutralized by immersing the slide in distilled water. Slides were dehydrated in serial dilutions of ethanol and the cover slipped with permount.

Bassoon Stain

Bassoon is a protein found in presynaptic neuron terminals and is thought to play a role in neurotransmitter release¹¹⁴. IHC staining for bassoon can label presynaptic terminals and differences in the number of presynaptic terminals may indicate changes in synaptic density resulting from PTN and PBS-treated rats. One slide of tissue per rat was dehydrated at 23°C for 20-minutes. Slides were washed for 10-minutes with PBS and 10-minutes in PBS with triton X-100 (PBS-Tx) @ 0.5%. They were then incubated for 1 hour in PBS-Tx containing 10% normal goat serum (NGS) and then with the primary antibody, mouse anti-bassoon, 1:400 (Enzo, SAP7F407), overnight at room temperature in PBS-Tx, 2% NGS. The following day, slides were washed 3x 10-minutes in PBS-Tx and then incubated for 2 hours with the fluorescence conjugated secondary antibody, goat anti-mouse AF647, 1:500 (Invitrogen, A28181). Slides were washed for 2x 10-minutes in PBS-Tx and then 2x 10-minutes in PBS, then the cover slipped with Fluoromount.

2.11 Neurite outgrowth and synaptic density analysis:

The bilateral CSTs were traced using AAV9s containing transgenes that express the fluorescent reporters GFP and tdTom to be able to visualize CST fibers in the spinal cord. One slide of tissue per rat was washed with PBS, coverslipped with flouromount, and then imaged using confocal microscopy (Leica DMI8 and TCS SP8). For the *PTN dose-response* experiment, images of three sections of tissue ~1 mm above and below the lesion site were imaged as a tile scan. For the *PTN vs. ChABC* and *PTN contusion SCI* experiments, spinal injection tracks were identified, and 5 sections of tissue were imaged as tile scans at these tracks and immediately surrounding these tracks. To quantify neurite outgrowth, an adapted version of the Sholl analysis¹¹⁵ was used to examine the density of CST traced fibres on the ipsilateral side. The number of AAV9 traced CST fibres crossing the midline and projecting into the contralateral grey matter was counted rostral and caudal to the injury both ipsilesional and contralesional. The average number of crossed fibres at each location from each group was used to compare differences in neurite outgrowth between groups.

An alternative approach to the neurite outgrowth analysis was taken for the *PTN DLQ SCI* experiment. Specifically, as a first step, the location of the spinal injection was identified using the DAB stain protocol described. Next, one section of spinal tissue was imaged at the injection site (C5), one section of tissue was imaged from the most caudal tissue sections on the tissue slide (~C6), and one section was imaged from the rostral most tissue section on the tissue slide (~C2-C3). For each section, the grey matter was then divided into three areas bilaterally: 1) the dorsal horn (DH), 2) the intermediate horn (IH), and 3) the ventral horn (VH). To delineate these regions, a horizontal line was drawn across the grey matter at the most ventral and midline area

of the grey matter and a second horizontal line was drawn at the point when the CST begins to diverge from the grey matter (Figure 10A). The grey matter ventral to the first horizontal line forms the VH, the grey matter ventral to the second horizontal line forms the IH, and the grey matter dorsal to the second horizontal line forms the DH. The intensity of the AAV9-tdTom and AAV9-GFP tracers were compared between the injured and non-injured sides in each of these 3 areas for each section of tissue. The mean intensity value of the ipsilesional side was divided by the contralateral side for each area. A ratio greater than 1 indicates the marker is more prevalent on the ipsilesional side and vice versa. The same analysis was conducted for the Bassoon IHC stain to measure changes in synaptic density between PTN- and PBS-treated rats.

Heat Mapping of CST axon density in the grey matter

A heatmap software developed by our laboratory was used to visualize neurite outgrowth in the *PTN dose-response* experiment. Three tissue sections imaged using confocal microscopy were uploaded onto ImageJ and an ImageJ macro was used to convert each pixel of a traced CST fibre within the grey matter into a coordinate location. These coordinates were saved as a data text file and these text files were then uploaded onto a script written in R. The R script takes the coordinates of the traced CST fibres within a group and overlays them to generate a density-based heat map. A heatmap highlights areas in the spinal grey matter that have different densities of CST fibres between groups and differences in sprouting between treatment groups can be visually inspected. The density heatmaps from each rat were normalized to the number of manually counted CST fibres traced in each rat (*normalization = pixel intensity / # of traced fiber*).

2.12 Statistical analysis:

All statistical analyses were performed with Graphpad Prism 9 Software (v9.1.2). Normality was assessed using the Shapiro-Wilk test when the number of rats per group was 4 and the D'Agostino & Pearson test when the number of animals per group was 8 or greater. For the horizontal ladder, von Frey hair test, and SPG task, a 2-way ANOVA test was used to examine whether there was a significant difference between PBS-treated and PTN-treated rats at any time point. When a significant difference between groups was identified, Tukey's multiple comparison test (when comparisons were made between multiple treatment groups at different time points) or Šídák's multiple comparisons test (when comparisons were made between 2 treatment groups (t-statistic) at different time points) was used to determine which experimental group differs from the rest. An unpaired t-test was used for lesion analysis and high-speed SPG analysis when 2 experimental groups were being compared. A 1-way ANOVA was used for lesion analysis when multiple treatment groups were being compared and for the *PTN In Vitro experiment* to compare length of neurite extension between treatment groups. Tukey's multiple comparison test was used to determine the groups between which there was a significant difference following the 1-way ANOVA. For the analysis of midline crossing fibres in the PTN contusion SCI experiment, normality could not be assumed, therefore, the Kruskal Wallis test was used.

Chapter 3: Results

3.1 PTN *in vitro* experiment: PTN promotes neurite outgrowth *in vitro*

It was important to first establish that our supply of PTN was active and could promote neurite outgrowth at a level similar to what has been reported in the literature⁹¹ and prior to administering PTN in *in vivo* models of SCI. We first tested the effects of our PTN supply *in vitro*. PTN was applied to rat cortical neurons plated on different concentrations of CSPGs bound to laminin and neurite outgrowth length was measured (in pixels). The application of cortical neurons onto CSPG coated plates significantly hindered neurite outgrowth (laminin 44.38 ± 3.83 ; laminin + low CSPG 22.19 ± 11.56 , $p < 0.05$; laminin + high CSPGs 11.27 ± 5.99 , $p < 0.0001$) (Figure 2B). The neurite outgrowth of cortical neurons grown on a low concentration of CSPGs with PTN was significantly higher than growth on low CSPGs alone (laminin + low CSPG 22.19 ± 11.56 , laminin + low CSPG + PTN 41.13 ± 9.60 , $p < 0.01$). The neurite outgrowth of cortical neurons grown on the high concentration of CSPGs with PTN was significantly higher than growth on high CSPGs alone (laminin + high CSPG 11.27 ± 5.99 , laminin + high CSPG + PTN 29.78 ± 5.95 , $p < 0.05$). These *in vitro* results indicated that our supply of PTN was active and capable of promoting neurite outgrowth. From these results, we felt comfortable moving forward with PTN experiments *in vivo*.

3.2 PTN vs. ChABC experiment: PTN promotes neurite outgrowth at a similar level to neurite outgrowth induced by ChABC

We proceeded to screen for the effects of PTN *in vivo* following SCI by comparing PTN to ChABC, a treatment known to promote neurite outgrowth with established protocols we could follow from published studies. Due to the ability of PTN to both neutralize CSPGs and upregulate growth promoting pathways within neurons, we hypothesized that PTN could

promote neurite outgrowth to a greater extent than ChABC treatment which only neutralizes CSPGs. To test our hypothesis, we used a DLQ model of SCI and compared PTN treatment to ChABC treatment targeted into the intermediate grey matter caudal and ipsilesional to the SCI. PTN and ChABC promoted more neurite outgrowth compared to PBS treated rats. However, contrary to our hypothesis, the number of midline crossing CST fibers was similar between PTN and ChABC treated rats caudal and ipsilesional to the SCI (Figure 3D) (PBS 0.06, PTN 0.12 ± 0.02 , ChABC 0.11 ± 0.03 , values represent the number of midline crossing fibers normalized to the number of CST axons traced in each rat). The number of rats per group was low (n=3), therefore, statistics were not run on this data. Regardless, this result provided evidence that our PTN could promote neurite outgrowth in our rat model of SCI, potentially at a level similar to ChABC, and we chose to proceed with larger *in vivo* PTN experiments.

3.3 PTN dose-response experiment: Higher doses of PTN may cause spinal cord damage

PTN and ChABC induced a similar extent of neurite outgrowth which raised the question of whether the effects of PTN is dose-dependent and a certain dose of PTN is needed to induce significant neurite outgrowth promoting effects. The *PTN dose-response* experiment was used to determine the optimal dose of PTN that would encourage neurite outgrowth but minimize potential side effects. Figure 4A shows representative cross-sections at the spinal PTN injection sites from rats receiving different concentrations of PTN. Injection tracks were visible in rats receiving 0.5 and 1.5 mg/mL concentrations of PTN however, rats that received 5 or 15 mg/mL concentrations had notable spinal tissue damage at the injection site, indicating potential PTN toxicity at higher concentrations. Figure 4B shows the area of damage at the SCI epicentre in each rat and the average area of damage is compared between treatment groups. There was a

general upward trend in the total area of SCI as the concentration of PTN administered increased. The total spinal cord area injured was significantly different between the PBS and 15mg/mL groups ($23\% \pm 10\%$ and $40\% \pm 6\%$, respectively; $p < 0.01$) and the 0.5 and 15 mg/ml groups ($24\% \pm 8\%$ and $40\% \pm 6\%$, respectively; $p < 0.05$). In rats treated with 5 and 15 mg/mL concentration of PTN, the injection damage overlapped with the SCI which may have contributed to the greater area of damage at the SCI epicenter. Based on these results, we concluded that PTN may damage spinal cord tissue in a concentration-dependent manner and PTN at lower concentrations should be used for subsequent experiments.

3.4 PTN dose-response experiment: PTN does not adversely alter forepaw sensation or long-term motor performance

An optimal dose of PTN would not only promote neurite outgrowth, but also minimize side effects. As such, von Frey hairs were used to assess for potential sensory changes resulting from different concentrations of PTN treatment (Figure 5A) and changes in motor performance was assessed using the horizontal ladder (Figure 5B). Motor and sensory data from male and female rats were combined because there was no significant difference between sexes in either the horizontal ladder task (p -value at baseline 0.99, week 1 0.49, week 3 0.07, week 5 0.52) or the Von Frey hair assessment (p -value right paw at week 1 0.99, week 3 >0.99 , week 5 0.98, week 7 >0.99 ; p -value left paw at all weeks >0.99) and this provided a larger n per group. From the von Frey assessment, we detected no hypersensitivity or allodynia resulting from PTN treatment regardless of the concentration used and the extent of spinal cord damage sustained (from both the SCI itself and the potential PTN-induced damage). A 2-way ANOVA indicated no significant differences in sensory function between rats treated with different concentrations of PTN at each timepoint following the SCI and spinal injections. In the horizontal ladder assessment, rats

receiving 15 mg/mL performed significantly worse than PBS-treated rats at 1-week post-SCI ($46.65\% \pm 19.01\%$ and $20.78\% \pm 16.44\%$, respectively; p -value <0.01), however, their performance improved by week 3 to a level similar to the other groups. By weeks 3 and 5, the percentage of missteps was not significantly different between any groups despite differences in total lesioned area. These results indicate that PTN treatment at any concentration does not cause significant changes to sensory function or long-term motor function.

3.5 PTN dose-response experiment: PTN-induced neurite outgrowth is dose-dependent and may differ between sexes

Neurite outgrowth was quantified at each concentration of PTN administered to determine the optimal dose of PTN to encourage neurite outgrowth. Both males and females were tested to see whether sex would affect the extent of neurite outgrowth. Neurite outgrowth was analyzed using a heatmap software to visualize the density of traced CST fibres in the grey matter (Figure 6).

Visual inspection of these heatmaps indicated a general upward trend in the density of traced fibres with increasing PTN concentrations in male rats. PBS-treated male rats had the lowest density. The density increased in the 0.5 and 1.5 mg/mL concentrations in male rats and was the highest at 5 and 15 mg/mL. Similarly, visual inspection of heatmaps from the female rats indicated a higher density of traced fibres at the 5 and 15 mg/mL concentrations of PTN.

However, the 1.5 mg/mL group showed the lowest density of traced CST fibres and the PBS and the 0.5 mg/mL groups showed a similar density of traced fibres. Therefore, the concentration of PTN administered alters the quantity of neurite outgrowth from the CST and there may be some dichotomy in neurite outgrowth between sexes following SCI and PTN treatment. Our results did not indicate a clear dose of PTN to use moving forward. We chose to proceed using PTN at a concentration of ~ 1.0 mg/mL because this dose elicited neurite outgrowth at a level similar to

ChABC in our previous experiment. This concentration of PTN was also used in the experiments published by Paveliev et al., 2016⁹¹ and Kuleskaya et al., 2021⁹².

3.6 PTN contusion SCI experiment: PTN-treated rats performed worse than PBS-treated rats in the SPG task

We next conducted the *PTN contusion SCI experiment* which combined PTN treatment targeted bilaterally rostral and caudal to the SCI with SPG training. This experiment aimed to assess for differences in neurite outgrowth between locations of PTN administration surrounding the SCI and whether PTN treatment and SPG training would have additive benefits on functional recovery. Starting with the effects of PTN on SPG training, our results showed that PTN-treated rats recovered to $16.5\% \pm 16.5\%$ of their success rate from baseline and plateaued in their recovery by week 3 (Figure 7A). Conversely, CTRL rats receiving only training after the SCI plateaued at 6 weeks post-SCI with a recovery of $44.8\% \pm 55.0\%$ from baseline. The success rate from baseline of CTRL rats and PTN-treated rats was significantly different at week 6 (PTN $10.8\% \pm 15.2\%$, CTRL $44.8\% \pm 55.0\%$). Using high-speed videography, the reaching and grasping technique of each rat post-SCI was compared to their baseline performance (Figure 7B). PTN-treated rats performed notably worse in the pronation and grasping component of the SPG task with a higher percentage of change from baseline ($-53.6\% \pm 31.8\%$; $-36.1\% \pm 64.2\%$, respectively) compared to their CTRL counterparts ($39.1\% \pm 35.3\%$; $-8.9\% \pm 87.7\%$, respectively). A lesion analysis was conducted to ensure the difference in SPG success rate and high-speed SPG performance compared to baseline performance was not due to significant differences in SCI lesion size. There was no significant difference in SCI size between treatment groups (CTRL $50.4\% \pm 9.1\%$, PTN $47.5\% \pm 4.2\%$). PTN did not induce any additional spinal cord tissue damage at the injection sites compared to PBS treated rats upon visual inspection. It

is unlikely that the spinal injections and damage sustained to the spinal cord through the SCI to be the underlying cause of the difference in SPG and high-speed performance (Figure 7C).

3.7 PTN contusion SCI experiment: changes in midline crossing CST fibers did not correlate to the poorer SPG performance of PTN treated rats

Midline crossing CST fibres were quantified bilaterally rostral and caudal to the SCI to see the effects of PTN targeted to different locations in the spinal cord and whether differences in the quantity of midline crossing fibers between PTN- and PBS-treated rats could potentially explain the difference in SPG outcomes (Figure 8B). PTN was administered bilaterally rostral and caudal to the SCI to encourage neurite outgrowth from both spared and injured axons surrounding the SCI in attempt to rewire the spinal cord to bypass the injury site. The quantity of midline crossing fibres at the injection sites rostral and caudal to the injury site were similar for both GFP and tdTom traced CST fibres between PTN- and PBS-treated rats (GFP rostral: CTRL 1.03 ± 0.67 , PTN 0.99 ± 0.35 ; GFP caudal: CTRL 10.40 ± 9.04 , PTN 10.21 ± 7.77 ; tdTom rostral: CTRL 1.003 ± 0.84 , PTN 1.72 ± 1.30 ; tdTom caudal: CTRL 5.95 ± 7.73 , PTN 5.117 ± 5.67). An increase in midline crossing fibers is associated with rewiring of neurons around the injury site. However, our results indicated no difference in midline crossing CST fibers between PTN- and PBS-treated rats. As such, the anatomical changes underlying the poorer performance of PTN treated rats remains unclear.

3.8 PTN DLQ SCI experiment: PTN-treated rats with a DLQ SCI performed worse than PBS-treated rats in the SPG task

To help elucidate the anatomical and/or physiological cause(s) underlying the poorer SPG performance of PTN treated rats compared to PBS-treated rats in the *PTN Contusion SCI* experiment, we simplified our experimental design in the *PTN DLQ SCI experiment*. We moved

to a DLQ model of SCI as it creates a more reproducible lesion between rats and better supports hypothesis testing. In addition to changing the SCI model, spinal injections for DLQ injured rats occurred 13-days after the SCI surgery (contusion injured rats received their injections at the time of the SCI surgery). A gap between the time of SCI and PTN and PBS injections was intended to give our rats more time to recover from the SCI before receiving spinal injections as rats in the PTN contusion SCI experiment were slow to recover. Similar to *PTN contusion SCI experiment*, rats with a DLQ injury treated with PTN appear to have performed worse in the SPG task compared to PBS-treated rats however, the performance of PTN treated rats was not significantly different from that of PBS treated rats at any time point (Figure 9A). PTN-treated rats plateaued at week 5 ($78.0\% \pm 42.9\%$) and PBS-treated rats plateaued at week 4 with a higher average score ($96.2\% \pm 35.8\%$). The reaching and grasping technique of each rat was scored using high-speed analysis (Figure 9B). PTN-treated rats had a larger percent change from baseline on all components following the ‘aim’ component of the high-speed analysis. The ‘grasp’ component of the analysis had the largest change from baseline. However, there were no significant differences in any component between the PTN and CTRL groups. The differences in SPG performance and reaching and grasping ability were not due to differences in lesion size between treatment groups (CTRL $26.37\% \pm 8.51\%$ and PTN $22.93\% \pm 6.90\%$) (Figure 9C). PTN- and PBS- were co-injected with BDA in this experiment to be able to accurately identify the of spinal injections. Visual inspection of spinal tissue at the injection sites did not show any additional tissue damage in PTN-treated rats compared to PBS-treated rats. Our results indicate that PTN treated rats performed worse than PBS-treated rats in the SPG task, although not significant at any timepoint. It is unlikely that the spinal injections or differences in SCI damage

between PTN- and PBS-treated rats could account for the difference in SPG performance between PBS and PTN experimental groups.

3.9 PTN DLQ SCI experiment: PTN-treated rats had more GFP traced CST fibres in the dorsal horn ipsilesional compared to CTRL rats

In this experiment, we took an alternative approach to quantifying AAV9 traced CST fibers to see if another neurite outgrowth outcome measure could better identify anatomical changes underlying our SPG training results. To examine whether PTN treatment had an effect on neurite outgrowth in the spinal grey matter, the tracing intensity of AAV9-GFP (ipsilesional CST) and tdTom (contralesional CST) was quantified and compared to PBS treated rats. In this experiment, PTN was only administered ipsilesional and caudal to the SCI to target spared axons caudal to the SCI and promote rewiring of neuronal circuits into the denervated region of the spinal cord. Neurite outgrowth was assessed rostral to the SCI (C2-3), at the spinal injection site (C5), and caudal to the injection site (C6) (Figure 10 B-G). At each location, the spinal grey matter was divided into three regions, VH, IH, and DH. To assess the extent of neurite outgrowth from the CST, the spinal grey matter on the ipsilesional side was compared to the intensity of CST sprouting in the contralateral grey matter to generate a ratio (i.e., ipsilesional: contralesional). A ratio greater than 1 indicates that the intensity of that tracer is greater on the ipsilesional side. GFP tracing was significantly less in PTN-treated rats in the VH caudal to the injection site compared to CTRL rats (CTRL 5.95 ± 5.75 , PTN 3.72 ± 2.76 ; * $P < 0.05$) (Figure 10G). At all other locations, there were no significant differences in tdTom or GFP traced CST fibres in the DH and IH nor tdTom in the DH (Figure 10 B-E and G) (tdTom rostral DH CTRL 0.03 ± 0.02 , PTN 0.06 ± 0.08 ; tdTom rostral IH CTRL 0.03 ± 0.02 , PTN 0.07 ± 0.04 ; tdTom rostral VH CTRL 0.22 ± 0.16 , PTN 0.18 ± 0.10 ; tdTom injection site DH CTRL 0.021 ± 0.02 ,

PTN 0.04 ± 0.04 ; tdTom injection site IH CTRL 0.10 ± 0.07 , PTN 0.06 ± 0.03 ; tdTom injection site VH CTRL 0.17 ± 0.13 , PTN 0.23 ± 0.17 ; tdTom caudal DH CTRL 0.01 ± 0.01 , PTN 0.04 ± 0.04 ; tdTom caudal IH CTRL 0.09 ± 0.06 , PTN 0.05 ± 0.04 ; tdTom caudal VH CTRL 0.18 ± 0.12 , PTN 0.19 ± 0.20 ; GFP rostral DH CTRL 40.8 ± 30.82 , PTN 70.53 ± 43.78 ; GFP rostral IH CTRL 54.32 ± 46.16 , PTN 43.08 ± 31.79 ; GFP rostral VH CTRL 10.91 ± 7.87 , PTN 10.76 ± 9.65 ; GFP injection site DH CTRL 33.14 ± 19.13 , PTN 47.64 ± 49.31 ; GFP injection site IH CTRL 23.87 ± 19.0 , PTN 36.92 ± 40.5 ; GFP injection site VH CTRL 5.35 ± 5.71 , PTN $7.06 \pm 4/19$; GFP caudal DH CTRL 45.37 ± 36.8 , PTN 20.01 ± 21.71 ; GFP caudal IH CTRL 30.02 ± 28.98 , PTN 26.61 ± 19.59).

3.10 PTN DLQ SCI experiment: PTN-treated rats had less synaptic density in the VH compared to CTRL rats ipsilesional and caudal to the spinal injection site

To extend our anatomical analysis beyond measuring changes neurite outgrowth in the spinal grey matter, we used bassoon IHC to visualize presynaptic terminals in PTN and PBS-treated rats as an alternative marker of spinal plasticity following SCI. The density of presynaptic terminals was compared between PTN- and PBS-treated rats to assess for any changes in synaptic density in the spinal grey matter. In the VH caudal to the spinal injection, the intensity of bassoon staining was significantly higher in the spinal grey matter contralateral to the SCI compared to the ipsilesional side in PTN-treated rats (Figure 10J). In contrast, CTRL rats had a greater bassoon intensity on the ipsilesional side in the VH (PTN 0.86 ± 0.27 , CTRL 1.15 ± 0.23 ; * $P < 0.05$). There were no significant differences in bassoon intensity in the DH, IH, and VH rostral to the SCI and at the injection site (Figure 10H and I) (rostral DH CTRL 1.22 ± 0.32 , PTN 1.17 ± 0.42 ; rostral IH CTRL 1.18 ± 0.22 , PTN 1.08 ± 0.27 ; rostral VH CTRL 1.26 ± 0.61 , PTN

1.02 ± 0.39; injection site DH CTRL 0.99 ± 0.37, PTN 1.0 ± 0.28; injection site IH CTRL 1.07 ± 0.22, PTN 1.05 ± 0.20; injection site VH CTRL 1.14 ± 0.25, PTN 1.02 ± 0.28; caudal DH CTRL 1.27 ± 0.25, PTN 1.03 ± 0.25; caudal IH CTRL 1.17 ± 0.26, PTN 0.99 ± 0.17).

Chapter 4: Discussion

The present studies aimed to examine the neurite outgrowth promoting effects of PTN and whether this neurite outgrowth could enhance functional recovery in rat models of SCI. In the *PTN in vitro* experiment, we showed that our supply of PTN was able to promote neurite outgrowth *in vitro* and in the *PTN vs. ChABC* experiment, PTN could promote neurite outgrowth *in vivo*. PTN increased neurite outgrowth in the spinal cord at a level similar to ChABC, contrary to our hypothesis that PTN would exceed the neurite outgrowth capacity of ChABC. Regardless, our preliminary studies indicated that our supply of PTN could promote neurite outgrowth and we moved forward with larger *in vivo* experiments. A PTN dose-response experiment was conducted to determine an optimal dose of PTN to promote neurite outgrowth and minimize side effects. Our results demonstrated that PTN administered at high concentrations can cause spinal cord tissue damage, however, there was no allodynia or hypersensitivity that resulted from PTN treatment. Additionally, PTN treatment induced different extents of neurite outgrowth at different concentrations and between sexes. As such, the results from our dose-response experiment did not clearly indicate a dose of PTN to proceed with for subsequent experiments. We chose to proceed with PTN at a concentration of ~1.0 mg/mL in subsequent experiments as this concentration promoted neurite outgrowth in our PTN vs. ChABC experiment and is the concentration used in published studies^{91,92}. Using this concentration of PTN, we conducted two more sets of PTN experiments, a PTN contusion SCI experiment and PTN DLQ SCI experiment. Both experiments aimed to examine for differences in neurite outgrowth resulting from PTN treatment targeted to different locations in the spinal grey matter as well as for additive effects of combining PTN treatment with rehabilitative training using the SPG task. In the *PTN contusion SCI* experiment, PTN treatment was administered bilaterally rostral and caudal to the SCI in the

intermediate grey matter and in the *PTN DLQ SCI* experiment, PTN was administered only caudal and ipsilesional to the SCI. Both experiments indicated that PTN-treated rats performed worse on the SPG task compared to PBS-treated rats. However, the anatomical and/or physiological changes underlying the differences in SPG performance were unclear and further investigation is needed to understand potential causes of the poorer performance in PTN-treated rats.

4.1 PTN *in vitro*:

To ensure that our supply of PTN was able to promote neurite outgrowth similar to other published studies, we tested our supply of PTN on rat cortical neuron cultures. In our study, cortical neurons were plated on laminin (a component of the ECM known to support neurite outgrowth, (reviewed in Powell and Kleinman, 1997¹¹⁶) and laminin-bound CSPGs. PTN applied to neurons grown in the presence of laminin bound CSPGs overcame the CSPG induce inhibition on neurite outgrowth and cortical neurons showed increases in neurite length of ~100% at both high and low concentrations of CSPGs (Figure 5). Our *in vitro* results were consistent with other published studies showing the growth-promoting effects of PTN^{77,91,117}. For example, Paveliev et al., 2016⁹¹ showed that hippocampal neurons from E17 rats grown on CSPGs at 50 µg/mL with PTN at 10 ug/mL increased neurite outgrowth up to 350% greater than neurite outgrowth on CSPGs alone.

Soluble CSPGs were used as an experimental group in this experiment because there is evidence that neurons respond differently to laminin-bound CSPG versus soluble CSPGs¹¹⁸. Our results showed that PTN treatment, in the presence of soluble CSPGs, promoted extensive neurite outgrowth. However, an important caveat to this finding is that no control group for soluble

CSPGs was used to measure their inhibitory effect on neurite outgrowth in the absence of PTN treatment (data is not shown in Figure 2 for this reason). Regardless, in discussing the effects and capabilities of PTN, the idea that PTN induced neurite outgrowth may change depending on the conformation of CSPGs is an important concept to consider when deciding where PTN should be administered to promote neurite outgrowth. CSPGs are present within the glial scar as well as within the ECM of the spinal grey matter, such as the PNN, surrounding the glial scar. However, the structure and composition of CSPGs within the glial scar is different from that of the PNN or the ECM¹¹⁹ which may, in turn, affect the activity of PTN if its effects are dependent on the composition and conformation of CSPGs within different CNS components. If the CSPGs are the target of PTN treatment, and PTN treatment is affected by CSPG conformation, it would be important to determine the CSPG population to which PTN treatment should be targeted to be the most effective.

In summary, our *PTN in vitro* experiment demonstrated the neurite outgrowth promoting potential of our supply of PTN. As such, we moved forward with examining the effects of PTN *in vivo*.

4.2 Application of PTN compared to ChABC *in vivo*

There were 2 reasons for comparing PTN and ChABC *in vivo*: 1) to ensure PTN could promote neurite outgrowth *in vivo* in comparison to a well-established promotor of neurite outgrowth and 2) to observe for any differences between ChABC and PTN sprouting. PTN was compared to ChABC because both factors act to neutralize the inhibitory effects of CSPGs. However, PTN has the ability to both block growth inhibitory factors and activate growth-promoting pathways. In theory, this mechanism should give PTN a stronger neurite outgrowth promoting potential.

However, our results suggested that PTN-induced neurite outgrowth *in vivo* was similar to neurite outgrowth induced by ChABC treatment (Figure 6). A caveat to this finding is that the number of animals per group was low in this experiment (n=3). Given our preliminary findings, this experiment should be repeated with a larger number of rats per group to determine whether neurite outgrowth is similar between PTN and ChABC treatment. We did not perform this experiment with a larger 'n' because it was intended primarily to screen for the neurite outgrowth promoting effects of our supply of PTN was active *in vivo*.

ChABC induced neurite outgrowth is generally reported as a result of neutralizing growth inhibitory CSPGs. However, a recent study published by Day et al., 2020¹²⁰ reported that SH-SY5Y neuron cultures transfected with a plasmid encoding ChABC with an axon-targeted signal enhanced the ability of the axon to promote neurite outgrowth. Targeting ChABC treatment to the neuronal axon was associated with increased expression of β -integrins, a receptor that plays a role in neurite outgrowth by interacting with CNS extracellular matrix. ChABC treatment also decreased the expression of PTEN and RhoA. Their results indicate that ChABC may be capable of both neutralizing growth inhibitory factors and increasing the capacity of neurons to support neurite outgrowth, giving ChABC a dual mechanism of action similar to PTN. This finding could potentially explain the similar extent of neurite outgrowth observed between PTN and ChABC treated SCI rats.

In summary, PTN injected ipsilesional and caudal to the SCI promoted neurite outgrowth following an SCI and given these results, we felt comfortable moving forward with larger *in vivo* PTN experiments.

4.3 Dose-response experiment:

Our dose-response experiment aimed to determine an optimal dose of PTN to be used *in vivo*. An optimal dose would maximize neurite outgrowth in the spinal cord following an SCI and minimize any potential side effects resulting from PTN treatment. Previous studies focusing on the application of PTN in rodent models of SCI have applied PTN at a concentration of 1 mg/mL into the SCI site at the time of SCI^{91,92}. These studies have shown evidence of neurite outgrowth using this concentration however, the rationale behind using this concentration *in vivo* has not been explored. We also took the opportunity to examine for any potential differences in PTN activity between sexes by studying each dose of PTN in both male and female rats. By conducting a dose-response, we aimed to build an evidentiary foundation to support our dose of PTN in subsequent experiments.

From our dose-response experiment, we noted that PTN administered at higher concentrations (5 and 15 mg/mL; 15 and 45 μ g of PTN respectively) caused spinal cord damage at the injection sites that was not present in rats treated at lower concentrations (0.5 and 1.5 mg/mL) or in PBS treated rats. In studies conducted by Paveliev et al., 2016⁹¹ and Kuleskaya et al., 2021⁹², PTN was administered into the SCI site during the same surgery as the SCI at 1 mg/mL and a volume of 5 μ L and 7 μ L respectively, equating to 5 and 7 μ g of PTN. No additional spinal cord damage was reported in these studies which coincides with our results showing that doses of PTN below 15 μ g do not cause additional spinal cord damage. However, Paveliev et al., 2016⁹¹ also specifically tested for PTN toxicity by injecting 0.1, 1, and 10 mg/mL of PTN into the mouse cortex at a volume of 1.5 μ L (0.15, 1.5, and 15 μ g of PTN, respectively) and examining the cortical tissue for markers of apoptosis. In contrast to our findings in the rat spinal cord, no toxicity was reported in mice receiving 15 μ g of PTN. Cortical toxicity was not tested in our

dose-response experiment and perhaps, there is a difference in sensitivity to PTN between the spinal cord and brain or perhaps between rat and mouse models of SCI.

We also considered our spinal injection technique as a potential source of the additional spinal cord damage observed. We provided spinal injections at a volume of 1 μL over the course of 1-minute using glass capillaries pulled into a needle of $<1 \mu\text{m}$ in diameter. Fluid exerts pressure therefore, PTN or PBS injections can exert pressure onto the spinal cord and cause damage. Like wise, the speed of an injection can effect the pressure exerted on the spinal cord. The glass needle must also penetrate through the dura before inserting into the spinal cord. The dura is more elastic and stiff than the spinal cord itself^{121,122} and if the glass needles used were too blunt, it could make it difficult to penetrate the dura, causing compression of the spinal cord during injections. A lack of tissue damage at the injection site in studies by Paveliev et al., 2016⁹¹ compared to our studies could be that they administered PTN into the SCI site, after inducing a transection injury and spinal injection damage may have been masked by the SCI. Injecting into the SCI site would have also created a cavity for PTN to fill, reducing the pressure of the spinal injections on the spinal cord tissue. Additionally, the transection injury would have decreased the resistance to backflow from the spinal injections, potentially diluting the dose of PTN administered into the spinal cord. Regardless, we ruled out our spinal injection technique as a potential cause given that all rats received their injection using the same type of needle at the same volume of injection. Each injection was timed to occur over the same interval of time and the additional spinal cord damage was consistent within the 5 mg/mL and 15 mg/mL groups. Furthermore, other published studies injecting the same or larger volumes of fluid into the spinal cord do not report damage to the spinal cord tissue^{76,92,105}.

To further elucidate potential causes of spinal cord damage at the spinal injection site, we considered the role PTN plays in neuroinflammation. Inflammation in the spinal cord is a double-edged sword in that it can be neuroprotective in the context of SCI (e.g., the glial scar) and inducing inflammation following SCI has been associated with functional recovery due to the upregulation of neurite outgrowth promoting substances^{107,108}. However, inflammation can also damage spinal cord tissue and cause neuron and cell death in the spinal cord^{123,124}. The upregulation of PTN during adulthood is associated with inflammatory processes and disease¹²⁵⁻¹²⁷ and neurodegenerative disorders¹²⁸, among other conditions. PTN can enhance the migration of inflammatory cytokines to areas of tissue damage^{129,130} and recently, it has been shown that PTN regulates lipopolysaccharide (LPS) induced microglial activation, inducing neuroinflammation¹²⁵. This neuroinflammation contributed to the pathology of diseases including Parkinson's disease which involves the degeneration of neuronal systems in the brain¹³¹. Given the role PTN plays in neuroinflammation, it is possible that PTN treatment can induce neurite outgrowth but also modulate harmful inflammatory pathways when administered into the spinal cord, leading to the spinal tissue damage seen in rats receiving higher doses of PTN. While higher doses of PTN may cause overt tissue damage, it is also possible that PTN induces more subtle tissue damage at lower doses. For this reason, it could be worth investigation spinal cord tissue treated with PTN for signs of inflammatory damage in comparison to PBS treated rats.

Another important aspect of our dose-response study was to examine for any functional side effects of PTN treatment. Due to the extensive role of PTN in the body, our experiments administered PTN directly into the spinal cord to minimize the chances of systemic side effects. Our results showed that both PTN and PBS-treated rats were hypoalgesic following SCI using

the von Frey analysis as a higher threshold was required to elicit a sensory response compared to baseline testing. The pattern of sensory changes was similar between PBS and PTN-treated rats over 7 weeks post-SCI. Hypoalgesia could be expected following SCI due to the interruption of ascending pain modulating tracts, however, some studies reported allodynia or hyperalgesia following SCI^{132,133}. We also reported no benefits to or long-term deficits in motor function in PTN-treated rats on the horizontal ladder. Rats treated at 15 mg/mL performed worse on the horizontal ladder compared to PBS-treated rats 1 week post-SCI, presumably due to the greater extent of spinal damage from both the SCI itself and the effects of a high dose of PTN. However, their performance was similar to all other treatment groups by week 3. The motor results obtained from our dose-response experiment contrast the results recently published by Kuleskaya et al., 2021⁹². In this study, mice with a C5 hemisection treated with PTN retained their motor skills on the vertical screen test and cylinder test at a level similar to sham injured rats and demonstrated significant functional recovery compared to PBS treated rats. They hypothesized that PTN administration at the time of SCI blocked the enhanced neuron excitability in the somatosensory cortex (measured using BOLD imaging) that was detected in mice without PTN treatment. They also suggested that PTN treatment, which has been reported to enhance GABA_A signalling, may have compensated for the loss of descending inhibition from the cortex following an SCI. By modulating neuronal activity in the somatosensory cortex and within spinal circuits, PTN may have improved functional recovery in mice with SCI in tasks requiring sensory processing and feedback to perform the task. One potential explanation for the difference in results obtained between our experiment and those published by Kuleskaya et al., 2021⁹² could be the site of PTN administration in the spinal cord. The aforementioned studies administered PTN at the site of SCI whereas our dose-response experiment administered PTN

into the intermediate grey matter 1mm rostral and caudal to the SCI. Injecting PTN at the injection site would target CSPGs within the glial scar whereas PTN injected into the intermediate grey matter would target the CSPGs within the ECM, including the PNN. CSPGs at the glial scar surround the area of injury and block the regeneration of injured axons across the injury site²⁸. In comparison, CSPGs within the ECM act to stabilize neuronal circuitry within the spinal grey matter^{134,135}. Disrupting this circuitry enables neurons to form new connections around the injury site, and in essence, rewire the spinal cord to bypass the SCI site⁷⁶. Comparing the outcomes of PTN administration at the SCI site versus rostral and caudal to the SCI site would be important to continue assessing the effects of PTN treatment in future experiments.

PTN treatment was compared between male and female rats to assess for any potential differences in neurite outgrowth and functional outcomes. Previous studies have reported that sex-associated hormones such as estrogen and testosterone can influence recovery following an SCI due to their neuroprotective effects, role in neuroinflammation, and influence on apoptotic pathways¹³⁶⁻¹³⁸. A study by Datto et al., 2015¹³⁹, reported that female rats with a thoracic SCI had greater preservation of spinal grey and white matter compared to male rats and this led to improved locomotor performance following SCI. Conversely, in a meta-analysis conducted by Becker et al., 2016¹⁴⁰, male and female rats did not differ in any behavioural, histological, or neurochemical traits at any point in the female estrogen cycle. Sex differences in PTN expression have not been previously explored and whether PTN treatment could be affected by sex is unknown. Our PTN dose-response experiment indicated a difference in neurite outgrowth between male and female rats at each concentration. Neurite outgrowth increased in male rats with increasing PTN concentrations. Conversely, female rats had similar levels of neurite outgrowth in the PBS, 0.5 mg/mL, and 5 mg/mL concentrations with the lowest neurite

outgrowth occurring in the 1.5 mg/mL group and the greatest occurring in the 15 mg/mL group. A potential explanation for the anomalous neurite outgrowth results between sexes could be that the spinal injections were too close to the SCI causing PTN-treated spinal cord tissue to overlap with SCI tissue. Spinal cord tissue at the SCI site is often distorted affecting the quantity of neurite outgrowth that can be observed in the tissue. Alternatively, it could be that female reproductive hormones influenced neurite outgrowth differently than male reproductive hormones leading to differences in neurite outgrowth between sexes. Studies have shown that estrogen therapy induces neuroprotective effects on neurons at the site of SCI¹⁴¹. Testosterone has been shown to reduce the degeneration of spinal motor neurons following an SCI¹³⁶. Another point to consider is that the distribution and concentrations of CSPGs in the CNS may differ between male and female rats. For example, the PNN composition differs between brain regions in male and female rats¹⁴²⁻¹⁴⁴. However, the CSPG composition in the spinal cord between sexes has yet to be explored to confirm this explanation. Overall, these results indicate a potential difference in neurite outgrowth between sexes, however, it would be important to confirm these findings by repeating the experiments with a larger number of rats per group. The finding that neurite outgrowth may be different between sexes speaks to one of the pitfalls in the field of SCI research that preclinical studies rarely consider biological sex as a variable. Many studies have published findings that biological systems differ between men and women¹⁴⁵⁻¹⁴⁷ and these differences influence the physiological changes that occur after a CNS injury^{141,148,149}. Therefore, sex may be a crucial factor in the interpretation and generalizability of research results. Regardless, many factors including the cost and the inconvenience and feasibility of housing and caring for double the number of rats often overshadows the need to consider sex in preclinical studies.

The PTN dose-response neurite outgrowth heatmap data did not indicate a dose of PTN that should be used for subsequent experiments. From visual inspection of the heatmaps, female rats treated with 1.5 mg/mL of PTN, the dose that is most similar to the studies by Paveliev et al., 2016⁹¹, appeared to have a lower neurite outgrowth compared to all other doses of PTN administered. However, Paveliev et al., 2016⁹¹ showed regeneration of injured axons across the injury site when PTN was administered to the SCI site. The heatmaps of male rats treated with the 1.5 mg/mL concentration showed more neurite outgrowth compared to PBS treated rats but less than 5 and 15 mg/mL treated rats. Following the dose-response experiment, it was still unclear as to what dose of PTN to use. However, given the time constraints of my degree and with COVID restrictions in place, we chose to proceed with a dose of PTN between 1 and 1.5 mg/mL as these concentrations did not elicit additional spinal cord damage in our models of SCI and have demonstrated neurite outgrowth promoting effects in the literature.

4.4 PTN contusion SCI:

In this experiment, PTN was administered at 4 locations in the spinal cord, 2 injections rostral and 2 injections caudal to the SCI, ipsilesional and contralesional in a contusion model of SCI to analyze the differences in neurite outgrowth between the 4 locations and the impact of PTN treatment on rehabilitative training using the SPG task. Rodent contusion SCI models are considered the most clinically relevant model of SCI because it recapitulates the pathology of a human SCI more closely than other rodent SCI models (e.g., a transection SCI)⁴. PTN was administered at 4 locations in the spinal cord to determine if more extensive PTN treatment surrounding the SCI would be associated with greater sprouting and functional recovery. Several studies have shown that neurite outgrowth can occur from both injured and spared axons rostral and caudal to the SCI and this outgrowth was associated with functional recovery following

SCI^{62,97-103}. The administration of PTN to 4 spinal locations was also intended to characterize any differences in neurite outgrowth that could emerge between the 4 locations. One caveat to this experimental design is that it is unknown whether PTN could exert effects beyond the site of injection. Presently, no study has been conducted to examine the spread of PTN in the spinal cord, therefore, it is unknown whether PTN can spread beyond its site of injection and how far. Paveliev et al., 2016⁹¹ analyzed the spread of PTN through the mouse cortex after a prick injury to the brain. Their results showed that PTN could be detected in the brain using Western blotting, 20 days after injection into the cortex and the spread of PTN in the cortex at day 20 was ~500 µm from the injury site. In comparison, the spinal injections in our experiments were ~4-5mm apart from each other, minimizing the chances that PTN effects overlapped between locations. Regardless, it is important to consider whether the effects of PTN can be treated as separate if they are administered into different but neighbouring regions of the spinal cord.

Midline crossing CST fibres were used as our measure of neurite outgrowth for this experiment. There is strong evidence in the literature supporting an increase in midline crossing CST fibres following an SCI (and other CNS injuries) and their contribution to functional recovery¹⁰⁰⁻¹⁰³ making midline crossing fibres a strong marker of neurite outgrowth. Neurite outgrowth emerges from the intact (contralesional) CST and crosses the midline to reinnervate and rewire the neurons denervated by the SCI¹⁰⁰⁻¹⁰³. Interestingly, our results showed no differences in midline crossing fibres between PTN-treated and PBS-treated rats at any of the 4 locations of spinal injections. Sham surgery rats were not used as a control in this experiment, so it is unclear whether there was an increase in midline crossing fibres in response to the SCI alone (PBS-treated). A potential explanation for a lack of significant difference between PTN-treated and PBS-treated rats may be that PTN was unable to increase the extent of midline crossing fibres

beyond what was already triggered by the SCI¹⁰⁰ and SPG training¹⁰². Other considerations include the tracer used to label the CST and the method used to quantify midline crossing fibres. BDA and AAV9s are commonly used CST tracers. Our lab has significant experience using both tracers and, in our experience, the benefit of using AAV9s is that more CST axons are labelled compared to BDA which traces a smaller proportion of the total CST fibres (~10%). AAV9s therefore allow more axons can be visualized in the spinal cord. However, AAV9s need to be carefully titrated to ensure that the proportion of CST fibres traced is manageable as excess AAV9 tracing can overwhelm the ability to distinguish between individual axons. This is generally not a concern with BDA as it is a less potent tracer. In our analysis, it is possible that the volume of AAV9 being used is too high and overwhelming our ability to distinguish differences in neurite outgrowth between treatment groups or even between regions within the spinal cord. To quantify midline crossing fibres, we counted the number of axons crossing the midline and normalized this number to the number of CST axons traced per rat. Another approach that has been reported in the literature is to quantify the percentage of labelled CST axons on the ipsilesional side as a percentage of labelled CST axons on the contralesional side¹⁰². Modifications to our experimental design and data analysis could be considered in the future to ensure that our methods are not masking any potential treatment effects.

In contrast to our anatomical results, a difference in functional recovery was noted between PTN- and PBS-treated rats. PTN-treated rats recovered only to ~17% of their baseline performance whereas PBS-treated rats recovered to ~45%. The high-speed analysis showed that PTN-treated rats performed more poorly on the pronation and grasping components of the SPG task. Impaired grasping (digit flexion) is more strongly associated with lesions to the dorsolateral funiculi^{150,151}. While the total area of SCI damage was not significantly different between groups,

it could be that a higher proportion of rats in the PTN group sustained damage to the dorsolateral funiculi region during their contusion SCI. Conversely, an unidentified consequence of PTN treatment could be negatively affecting motor recovery. Similar to the discussion presented in section 4.3, PTN is involved in extensive processes throughout the human body, including processes that trigger damage or disease to the body. It is possible that unidentified consequences of PTN treatment (e.g., inflammation) maybe occurring at a cellular level in the spinal cord tissue that has not been detected during our methods of histological analysis for lesion size, IHC processing, and neurite outgrowth analyses. The disparity in motor performance between PTN and PBS-treated rats warrants further investigation.

4.5 PTN DLQ SCI:

With inconclusive anatomical results from the *PTN contusion SCI* experiment, we simplified the experimental design to help elucidate the cause underlying a worse functional outcome in PTN-treated rats. We moved to a DLQ model of SCI as it is a more reproducible lesion and a better option to support hypothesis testing. A single spinal injection was given caudal and ipsilesional to the SCI. The spinal injections were given 13 days after the SCI for three important reasons. First, delaying the spinal injections to allow the rats more time to recover after their SCI before administering spinal injections. Rats from the *PTN contusion SCI experiment* recovered slowly from their contusion SCI and 4 spinal injections, likely due to the complexity of the surgical procedures performed and the increased time under anesthesia to perform all of these procedures. Secondly, increasing the duration between SCI and treatment had the added benefit of making treatment injection more clinically relevant in this experiment. In a clinical setting, SCI treatments are typically not provided at the time of SCI but a period of time after once the patient's clinical status has been stabilized. Thirdly, CSPGs have been shown to be upregulated

at the site of SCI and in the lesion penumbra overtime^{28,152}. If one of the mechanisms through which PTN is thought to act is through CSPGs, therefore, administering PTN at a later time point could have added therapeutic benefit. To summarize, the experimental design for the PTN DLQ SCI experimental was simplified from the PTN Contusion SCI experiment to help investigate the mechanism (s) underlying the poorer SPG performance of PTN-treated rats compared to PBS-treated rats in the SPG task after SCI.

Rather than counting midline crossing fibres as was done in the *PTN contusion SCI* experiment, the analysis of midline crossing fibres was carried out by comparing the quantity of CST fibres on the ipsilesional side as a ratio to the contralesional side. Crossing fibres were analyzed rostral to the SCI, at the spinal injection site and caudal to the injection site. AAV9-tdTom was used to label the contralesional CST therefore, tdTom fibres on the ipsilesional side would represent intact CST fibres crossing the midline to form new connections on the denervated side of the spinal cord. Conversely, AAV9-GFP was used to label the ipsilesional CST so midline crossing fibres would indicate axons moving from the denervated side of the spinal cord towards intact CST axons. PTN treatment did not increase the quantity of midline crossing fibres targeting the denervated region of the spinal cord. This result contradicts published findings that neurite outgrowth promoting treatments encourage CST axons to cross the midline to innervate the denervated spinal cord region and facilitate motor recovery¹⁰⁰⁻¹⁰³. Conversely, GFP tracing was significantly lower in PTN treated rats caudal to the injection site in the dorsal horn. The dorsal horn is primarily responsible for relaying sensory information incoming from the periphery (reviewed by Harding et al., 2020¹⁵³). Interestingly, no significant differences were noted between PTN and PBS treated rats in the von Frey analysis despite significant changes in quantity of CST fibers in the dorsal horn caudal to the spinal injection site. These contradictory

findings may indicate that more sensitive measures of sensory changes should be used in future experiments such as the Hargreaves test¹⁵⁴ or hot plate test¹⁵⁵.

Changes to CST connections in the dorsal horn caudal to the PTN injection site could potentially underlie the poorer SPG performance in PTN treated rats. While SPG training is often viewed as a motor task, appropriate sensory input from the forepaw is required to provide feedback to the rat throughout the task (e.g., detect the pellet grasped in the forepaw)^{92,156} especially as the visual feedback is lacking/low due to limited eyesight in Lewis rats. We used von Frey hairs to measure sensory changes and our analysis indicated no sensory changes resulting from PTN treatment, however, von Frey hairs can be a subjective outcome measure and the sensitivity of the test can vary based on the experimenter, the environment in which it takes place, and the instruments used among other factors¹⁵⁷. Therefore, it is possible that changes in sensory detection were not detected by the von Frey hair assessment in our experiments. Changes in connectivity of the DH may coincide with our finding that PTN-treated rats also showed less presynaptic density ipsilesional to the SCI and caudal to the spinal injection site in the VH compared to PBS-treated rats. A significant change in presynaptic density may indicate PTN induced spinal circuit remodelling in the VH following SCI. The ventral horn of the spinal cord contains the cell bodies of motor neurons, and the cell bodies of motor neurons are surrounded by a dense PNN network, therefore, a potent target for PTN treatment^{158,159}. A decrease in synaptic density in the VH could indicate that PTN has disrupted the PNN surrounding the neuronal network in the VH, inducing spinal plasticity. Alterations to synaptic density in the VH could impair motor function in rats and if motor connectivity changes alongside changes in sensory connectivity in the DH, these alterations to sensory-motor systems could account for the poorer performance of PTN treated rats in the SPG task.

In summary, the *PTN DLQ SCI* experiment showed decreased CST fiber density in the DH ipsilesional and caudal to the spinal injection site as well as decreased synaptic density caudal and ipsilesional to the spinal injection. No consequences to sensory function were observed in PTN treated rats however, changes in neuronal connectivity in the VH and DH caudal to PTN treatment could potentially explain the SPG performance of PTN treated rats

4.6 Bringing together the anatomical and functional data across PTN experiments:

The anatomical changes, such as CST fiber density and synaptic density, underlying the differences in SPG training were inconclusive and the potential mechanisms causing PTN-treated rats to perform more poorly than PBS-treated rats. Moving forward, some considerations that should be made include taking more steps to determine where PTN should be applied in the CNS and determining if there are limits to the benefits of promoting plasticity in the spinal cord.

In my studies, the markers of neurite outgrowth used included the quantification of midline crossing fibres, the comparison of staining intensity between the ipsilesional and contralesional sides of the spinal cord, as well as bassoon IHC to identify presynaptic neuron terminals. Midline crossing fibres provided inconclusive results in the *PTN contusion SCI* experiment, as such, we moved to the comparison of the staining intensity between the ipsilesional and contralesional sides of the spinal cord, as well as bassoon IHC in the *PTN DLQ SCI* experiment. While these latter 2 approaches to analyzing neurite outgrowth demonstrated some changes in the distribution and quantity of neurites following PTN treatment, the results we obtained did not match our hypothesis that PTN would encourage significant neurite outgrowth in our models of SCI. Our *in vivo* PTN results also did not reflect the data published in the literature demonstrating significant neurite outgrowth promoting effects of PTN. There are many possible explanations for the

discrepancy between our current findings and published data including perhaps that our location of PTN administration was not maximizing the potential of PTN to promote neurite outgrowth or perhaps the combination of PTN treatment with rehabilitative training is not additive as we had hypothesized. As mentioned previously, published *in vivo* studies have previously administered PTN at the site of SCI⁹¹ whereas our current experiments administered PTN into the intermediate grey matter rostral and caudal to the SCI. CSPGs are a structural component of the PNN in the intermediate grey matter whereas, at the SCI site, CSPGs are deposited by astrocytes to seal off the site of injury. The quantity and organization of CSPGs between these two regions could potentially impact the effectiveness of PTN. My thesis aimed to only examine the effects of PTN administered rostral and/or caudal to the SCI. However, a study comparing neurite outgrowth resulting from PTN administered rostral and/or caudal to the SCI to PTN administered at the site of SCI could help elucidate whether the effectiveness of PTN differs between these locations.

Another important discussion to consider is that inducing neurite outgrowth may come with potential caveats. In our current studies, PTN-treated rats performed more poorly in the SPG task compared to PBS-treated rats. While the mechanism underlying the poor SPG performance is not clear, it raises the question of whether encouraging neurite outgrowth could negatively impact functional recovery following SCI. In our experiments, we administered PTN into the intermediate grey matter to disrupt CSPGs within the PNN that stabilizes neuronal networks. PNNs are upregulated following an SCI to prevent excitotoxicity of neurons and blocking the upregulation of PNNs using ChABC has been shown to lead to increased levels of cell death^{134,160}. These results could indicate that timing neurite outgrowth promoting treatments could be crucial to balancing the development of excitotoxicity with the induction of neurite outgrowth to improve functional recovery. In our *PTN DLQ SCI* experiment, we partly addressed

this concern by administering PTN treatment 13 days following the SCI. However, our PTN-treated rats still performed more poorly on the SPG task compared to PBS-treated rats, although the performance was better than the *PTN contusion SCI* rats treated at the time of SCI. PNNs also surround motor neurons in the VH of the spinal cord¹⁵⁸. Administering PTN to disrupt the PNN could, in theory, reopen the window for plasticity as demonstrated in Garcia-Alias et al., 2009⁷⁶. Conversely, disrupting the PNN surrounding motor neurons could also impair motor function. This hypothesis could potentially explain the poorer performance of PTN-treated rats on the SPG task. The concept that changes in neurite outgrowth or spinal plasticity can be maladaptive is not new. The development of allodynia or neurogenic pain following a SCI is associated with alterations to the DH of the spinal cord¹⁶¹. Not only is pain a negative consequence of spinal plasticity, but pain can also hinder functional recovery in rodent models of SCI¹⁶². Girgis et al., 2007⁶⁴ demonstrated that SPG training-induced neurite outgrowth in the spinal cord could lead to improvements in the SPG task performance however, this improvement came at the expense of an untrained task (e.g., the horizontal ladder). It is important to consider the caveats of neurite outgrowth promoting treatments such as PTN, to balance the potential to improve functional recovery following an SCI with the potential to impair functional recovery.

4.7 Future directions:

While I have presented many considerations moving forward with this series of PTN experiments, I believe the next logical step should be to establish the neurite outgrowth promoting effect of PTN *in vivo*. This experiment would apply PTN treatment to a DLQ model of SCI. PTN treatment targeted rostral and caudal to the SCI would be compared to PTN treatment targeted at the SCI site. Neurite outgrowth from PTN-treated rats would be compared to PBS-treated rats and sham injured rats using a variety of measures. Additionally, this

experiment would occur in the absence of rehabilitative training to simplify the experiment and remove a potential confounding factor. This study would aim to determine whether PTN is more effective at promoting neurite outgrowth at the injury site compared to around the injury site and whether PTN-induced neurite outgrowth in the spinal grey matter re-emerges in the absence of rehabilitative training. More complex experiments can be performed once the neurite outgrowth promoting effects of PTN have been established.

Chapter 5: Conclusion

My thesis aimed to explore the use of PTN as a neuroplasticity promoting treatment. Each experiment aimed to examine different aspects of the neurite outgrowth promoting capacity of PTN. The results obtained from my experiments indicate that PTN plays a role in neuroplasticity and that PTN can influence functional outcomes following a SCI. However, further investigation is required to determine what outcome measure best depicts the PTN induced plasticity and whether this plasticity is maladaptive and hinders functional improvement.

Chapter 6: The future of SCI research

In relation to my field of preclinical SCI research, advancements or new approaches to neurite outgrowth promoting treatments generally involve targeting multiple factors associated with growth promotion and/or growth inhibition to generate a combination treatment that bolsters neurite outgrowth beyond one single factor. This concept was also the focus of my thesis. For example, a recent study published by Hosseini et al., 2022 targeted CSPGs, LAR and PTP σ signalling pathways and NPCs all in one experiment¹⁶³. None of these molecules or pathways are new discoveries, in fact papers dated in the 1900s or earlier can be found regarding these molecules¹⁶⁴⁻¹⁶⁶. However, it is becoming increasingly realized that CNS recovery after an

injury involves such a multitude of factors that a single approach is not sufficient to repair the injured spinal cord. Another area of advancement in SCI research that goes hand-in-hand with the development of plasticity promoting treatments, is the development of non-invasive treatment delivery systems. One of these advancements is nanoparticle (NP) treatment delivery technology¹⁶⁷. NPs are structured such that they can be administered systemically (e.g., in the blood), avoid physiological systems intended to remove foreign substances from the body, cross the blood-brain barrier to target CNS structures, and then target specific cells of interest by attaching peptides onto their surface. Advancements in treatment delivery systems are important in the field of SCI where pharmacological treatments targeted into the spinal cord often require inducing another SCI to provide the treatment.

In the clinical world of SCI, many clinical trials listed by organizations such as the MayoClinic that are looking to improve functional outcomes after SCI involve rehabilitative training or along a similar mechanism, electrical stimulation. These studies are based on the idea that increasing activity within spared neuronal circuits will help rewire the spinal cord and recover function of specific body parts or recover function in specific tasks. There are also some clinical trials revolving around stem cell transplants to regenerate cells within the CNS after injury. Currently, there is a clinical trial that closely aligns with my preclinical work. This study assesses the efficacy and safety of MT-3921 in acute traumatic cervical SCI (NIH clinical trials data base, identifier NCT04683848). MT-3921 is a monoclonal antibody that binds repulsive guidance molecule A (RGMa), and they are assessing for changes in motor function of upper extremities. In the developing nervous system (RGMa) plays a role in guiding growth cone and axon trajectories through the CNS similar to CSPGs^{168,169}. This is an exciting development in clinical trials as it pertains closely to the principles underlying my preclinical research and may indicate

the advancement of pharmacological treatments studied in preclinical settings into clinical trials down the road.

SCI is a complex field of research because a SCI affects so many aspects of an individual's life from their mental health and their activities of daily living to changes in their physiological systems including their bladder and sexual function, and their physical activity. Preclinical SCI research models often do not account for many factors that influence recovery after SCI including the sex of the patient or the mental health of the patient. There has been a push towards considering more variables in preclinical models of SCI to improve the applicability and generalizability of SCI research data. For example, in 2015, the National Institute of Health announced that they expect scientists to better account for the possible role of sex in research studies¹⁷⁰. A recent development that may help with progressing SCI research and make it more feasible to account for the numerous variable that influence SCI recovery is the development of the Open Data Commons (ODC) for SCI research¹⁷¹. Data sharing would generate a repository of data whereby SCI researchers across the globe can access the data, generate more meaningful meta-analyses, and draw conclusions from a collection of data without having to produce the results themselves for each data set. The burden of including factors like mental health or sex in a research design no longer lies with an individual research group but rather, the entire SCI research community is responsible for generating and contributing to the Open Data Commons (ODC) and the goal to make SCI research more generalizable becomes more feasible. While I may not repeat my PTN dose-response examining the effects of sex on neurite outgrowth, researchers throughout the world studying PTN can build-off the study I initiated if I upload my data for them to access on the ODC. SCI research, and many other fields of research for that matter, will be advanced significantly from this development.

The field of SCI is constantly progressing, and I am hopeful for the future develop of SCI treatments to encourage spinal cord repair and improve the quality of life for those living with SCI.

Chapter 6: Figures

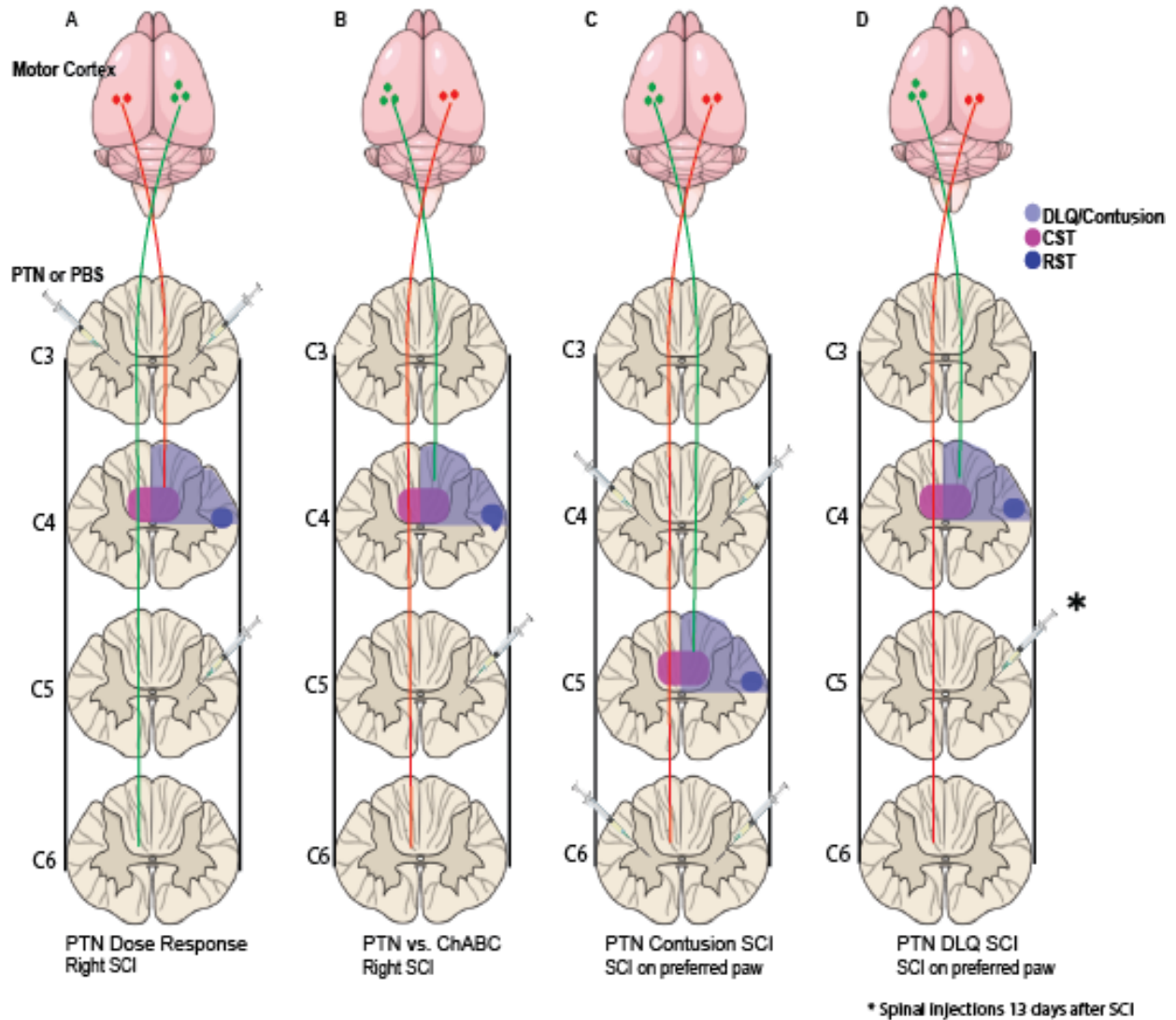
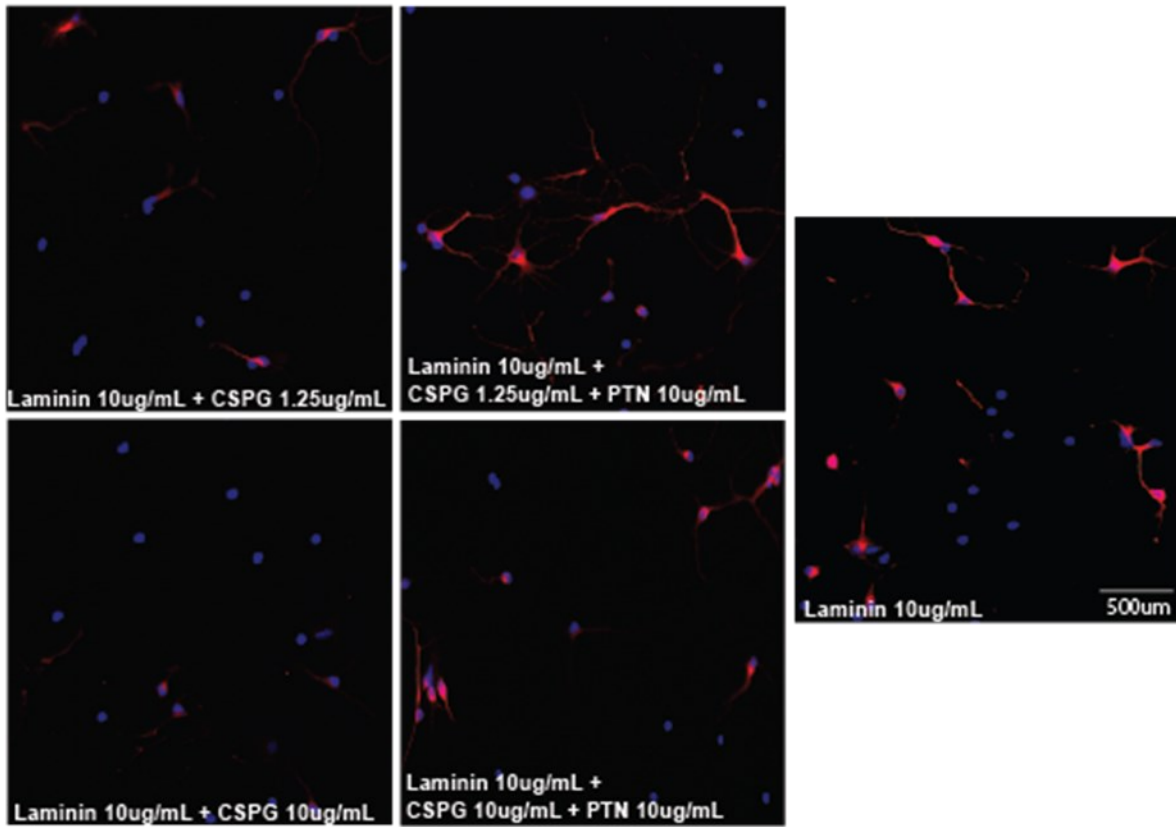


Figure 1: Schematics of rat SCI, spinal injections, and cortical injections for each experiment.

To help visualize the methods of each experiment involving a SCI, spinal injections, and cortical injections.

A



B

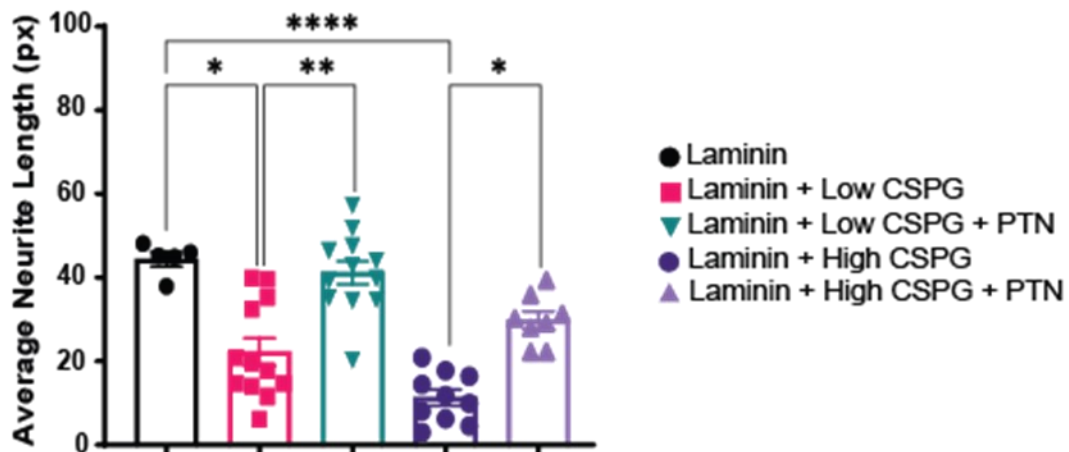


Figure 2: Application of PTN *in vitro*.

The growth of rat cortical neurons on laminin (10 $\mu\text{g}/\text{mL}$) and CSPGs at 1.25 and 10 $\mu\text{g}/\text{mL}$ in the presence or absence of PTN at 10 $\mu\text{g}/\text{mL}$. (A) Confocal images to visually compare the relative amount of neurite outgrowth of cortical neurons treated with different combinations of

substrates. (B) Quantification of neurite outgrowth. Neurite outgrowth on laminin was significantly greater than outgrowth on laminin + either concentration of CSPGs. The inhibition of growth on laminin by CSPGs was partly reversed by the addition of PTN. * $P \leq 0.05$, ** $P \leq 0.01$, *** $P \leq 0.0001$; error bars show the standard deviation.

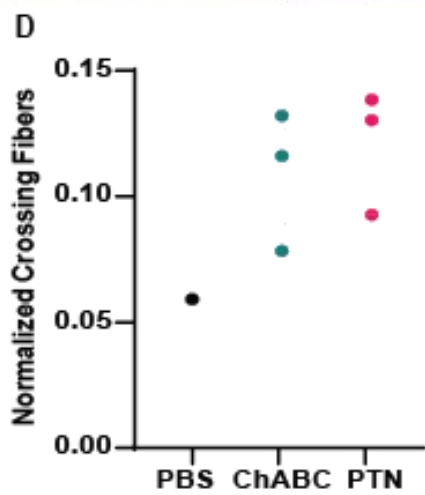
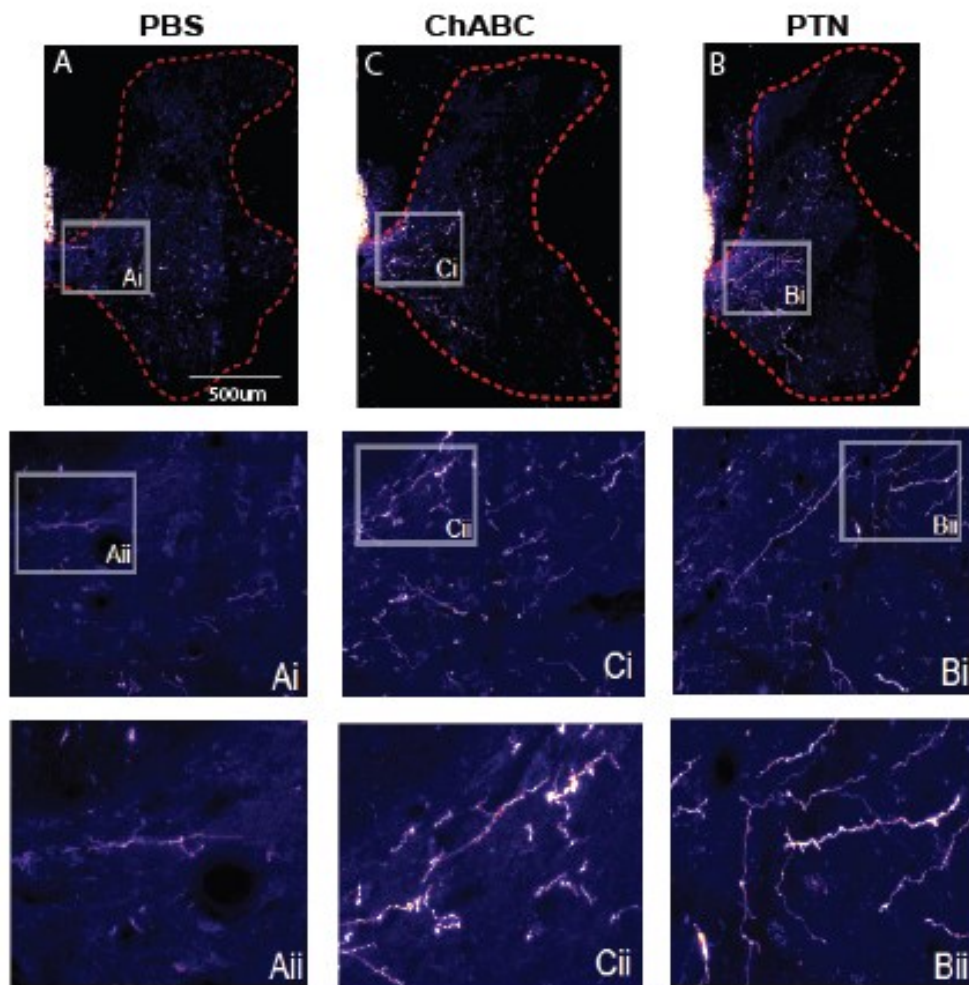


Figure 3: PTN promotes neurite outgrowth in vivo.

PTN-induced neurite outgrowth was compared to ChABC-induced neurite outgrowth to screen the neurite outgrowth promoting effects of PTN *in vivo*. (A-C) Spinal cross-sections showing the midline crossing CST fibres into the contralateral grey matter, traced with AAV9-tdTom, that were used to quantify neurite outgrowth. (D) Neurite outgrowth in PTN treated rats was similar to ChABC treated rats. The number of crossing fibres was counted per rat and normalized to the number of CST axons traced per rat. Both PTN and ChABC treated groups had a higher density of midline crossing CST fibres compared to PBS control rats. Error bars show the standard deviation.

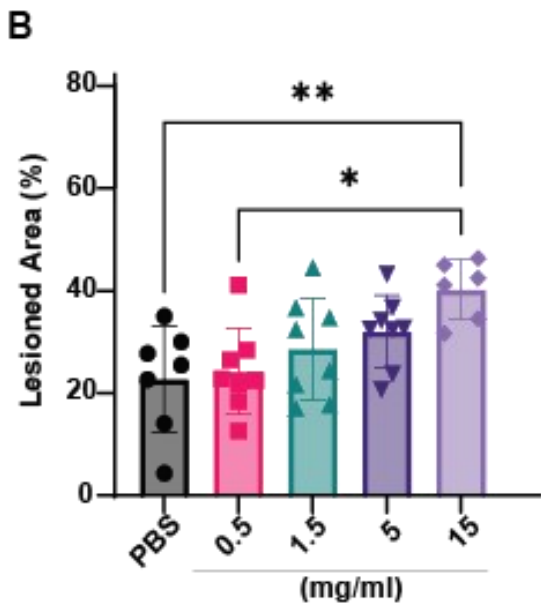
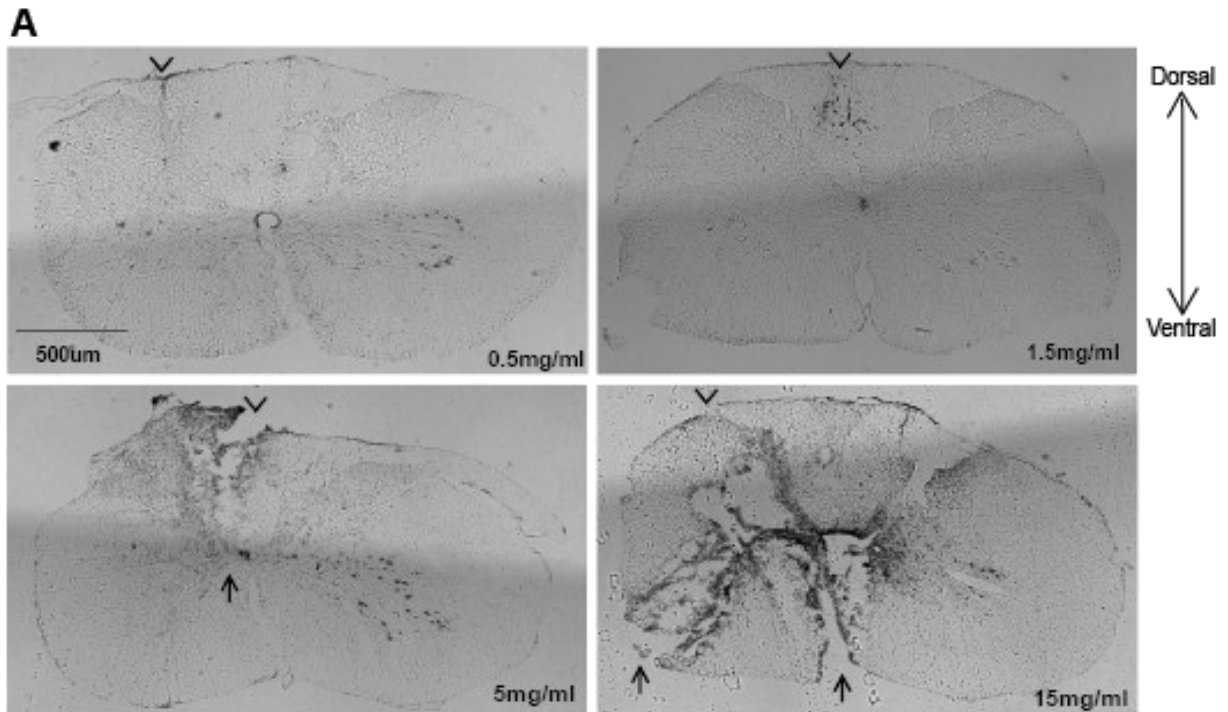


Figure 4: Anatomical results from the PTN dose-response experiment.

(A) Cross-sections of spinal cords at the spinal injection sites treated with cresyl violet stain from rats receiving different concentrations of PTN treatment. Rats receiving 5 and 15 mg/mL concentrations showed notable damage at the injection site compared to rats treated with lower

doses of PTN showing only injection tracts. Arrowheads indicate injection sites and arrows indicate areas of damage beyond the injection sites themselves. The faint shadow that runs diagonally across each image is an artifact of tilescan stitching on the brightfield microscope. (B) The area of spinal cord damage at the lesion epicenter presented as a percentage of the total area of the spinal cord. The percentage of damaged area was compared between treatment groups. An upward trend is noted as the concentration of PTN increases, with the lesioned area of the 15 mg/mL group significantly different than the PBS and 0.5 mg/mL groups. There was some overlap between SCI damage and injection damage in the 5 and 15 mg/mL groups. * $P \leq 0.05$, ** $P \leq 0.01$, error bars show the standard deviation.

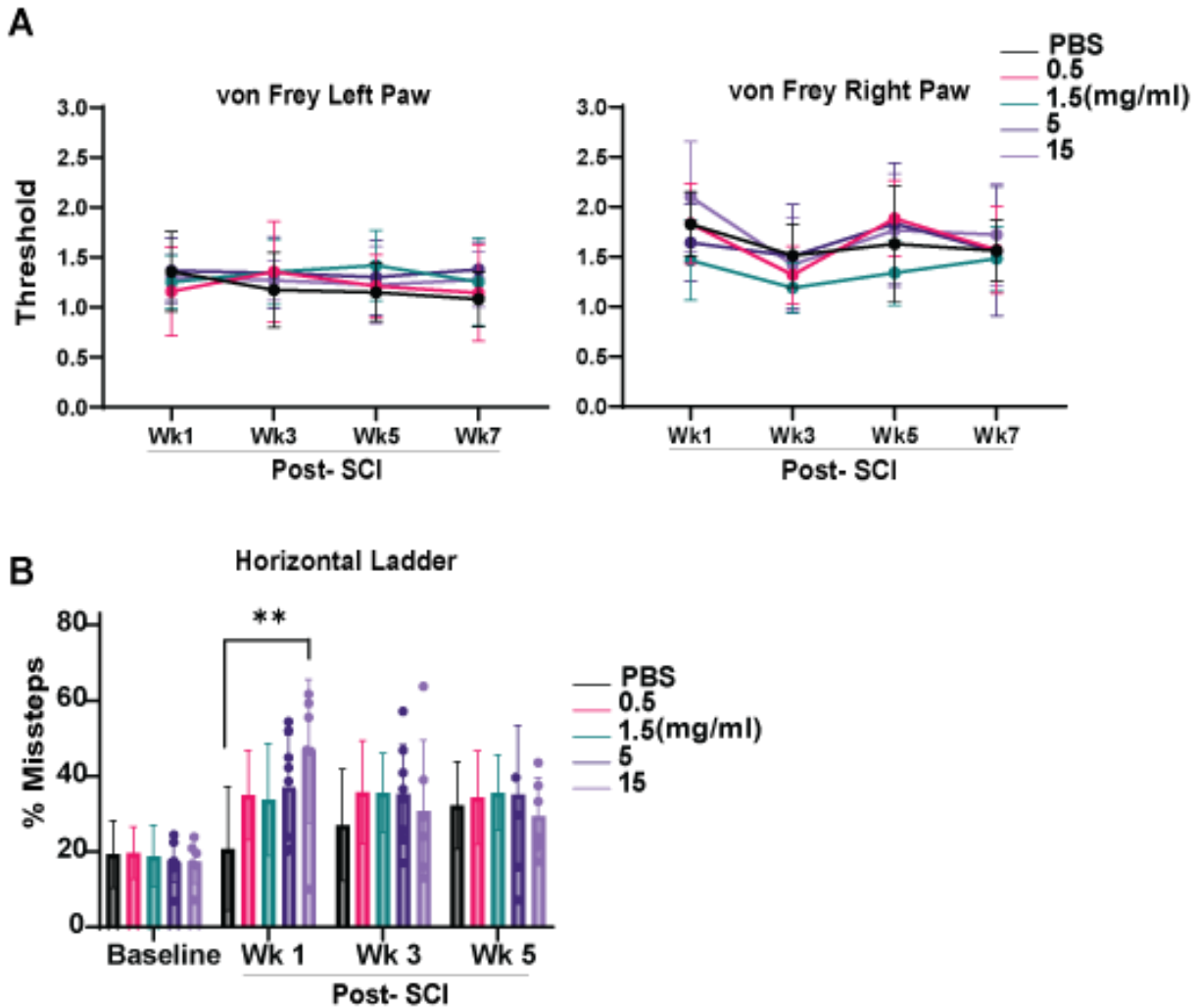
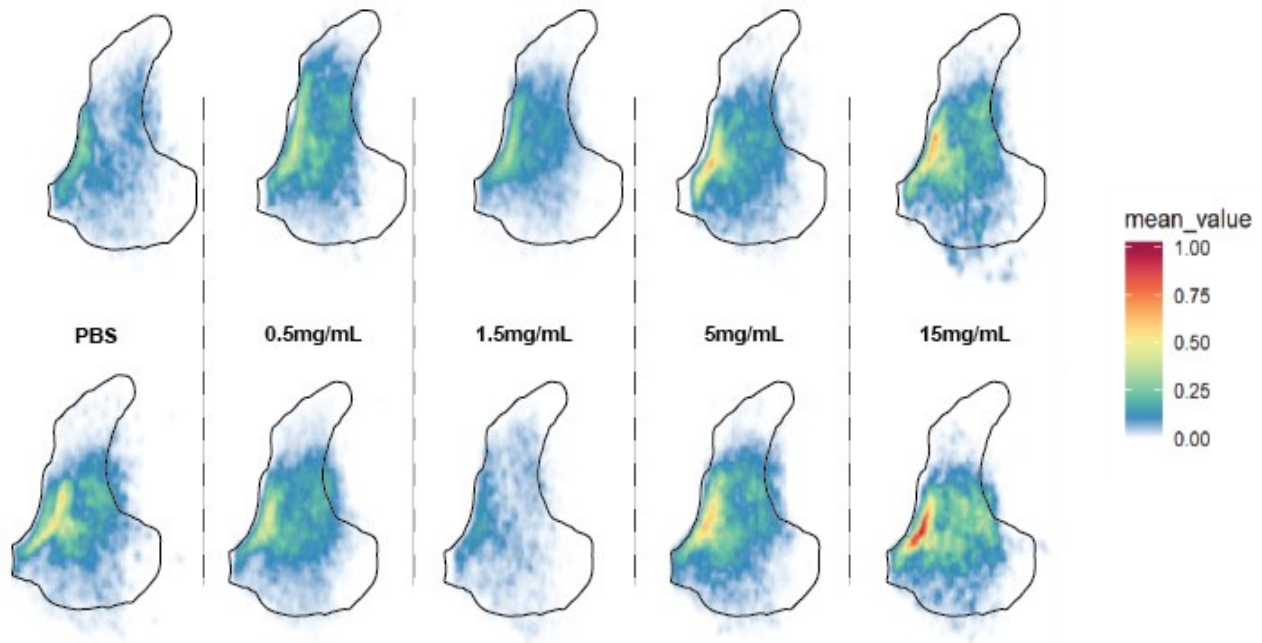


Figure 5: Sensory and motor changes noted during the PTN dose-response experiment.

Sensory and motor changes following PTN treatment were assessed using the von Frey hair test and the horizontal ladder. (A) The von Frey hair test data is presented as the threshold required to elicit a sensory response at 1,3, 5-, and 7 weeks post-SCI normalized to the threshold at baseline. Data showed that PTN-treated rats followed the same pattern of sensory changes as PBS-treated rats in both the right and left paw for 7 weeks post-SCI and PTN treatment. (B) Horizontal ladder assessment data are presented as the average % of forepaw missteps (slip or miss) within each

group compared between groups at 1,3-, and 5 weeks post-SCI. The motor performance was significantly different between PBS and 15 mg/mL treated groups at Wk 1 post-SCI but this difference was no longer apparent by Wk 3. $**P \leq 0.01$, error bars show the standard deviation.

Male TdTom (ipsilesional) CST fiber density



Female TdTom (ipsilesional) CST fiber density

Figure 6: PTN dose-response heatmaps. analysis.

Visual representation of the differences in neurite outgrowth at the ipsilesional rostral injection site. Heatmaps are compared between groups treated with different PTN concentrations within sex and the differences in neurite outgrowth at different concentrations between sexes. The intensity of pixels of traced CST fibres within the ipsilesional spinal grey matter was compared between groups. The heatmap provides the density of pixels (therefore, CST fibres) at different locations across the spinal grey matter. There is some dichotomy between male and female rats at different concentrations of PTN administered.

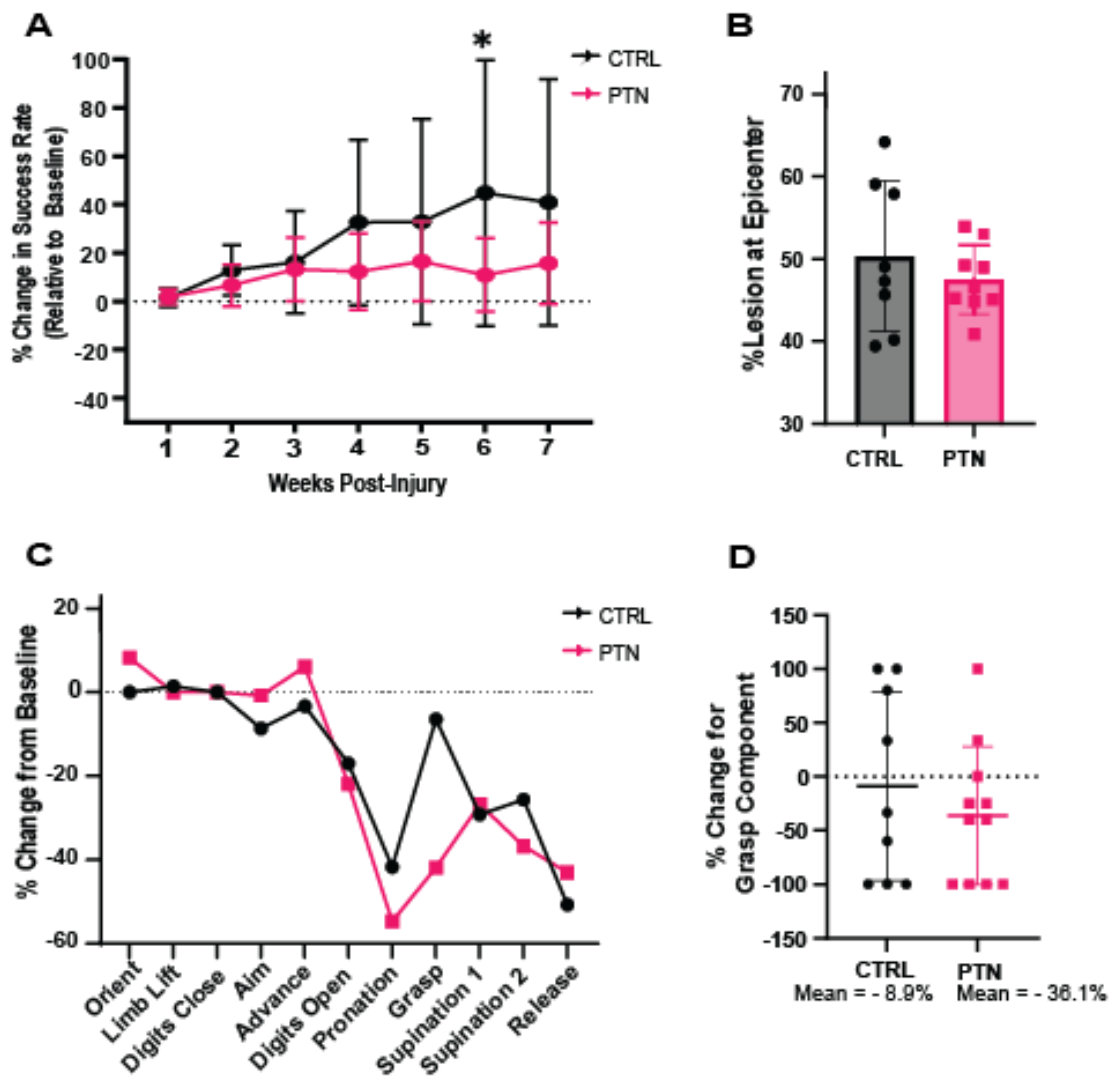


Figure 7: Outcome of rats with a contusion SCI treated with PTN and SPG training compared to PBS-treated rats.

(A) The SPG score of rats from weeks 1-7 post-SCI normalized to the highest SPG success score obtained pre-SCI. Rats treated with PTN recovered less than PBS-treated rats in the SPG task.

The difference in recovery was significant at week 6 post-SCI. (B) At the lesion epicentre, the area of total spinal cord damage was calculated as a percentage of the total spinal cross-section area. There was no significant difference in lesion size between PBS- and PTN-treated rats. (C)

Using the high-speed recordings rats were assessed on specific components of the SPG task at

baseline before SCI and post-SCI at the end of SPG training (week 7). The data is presented as the percentage change from baseline scores following SCI and PTN treatment. PTN-treated rats performed more poorly in the pronation and grasping component of the SPG task. *P<0.05; Error bars show the standard deviation. (D) Percent change values for PTN and CTRL rats for the grasping component of the high-speed analysis. The mean for the CTRL group is 8.9% and the mean for PTN group is -36.1%.

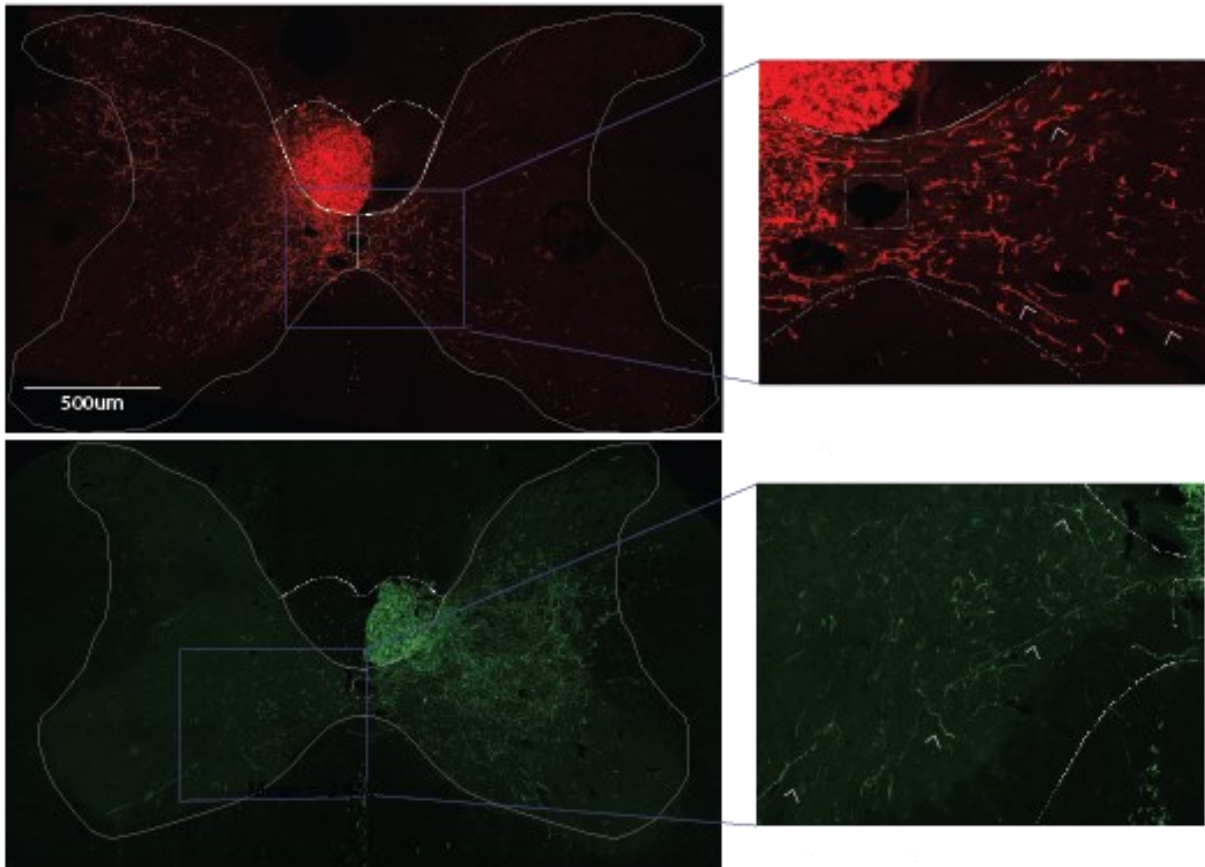
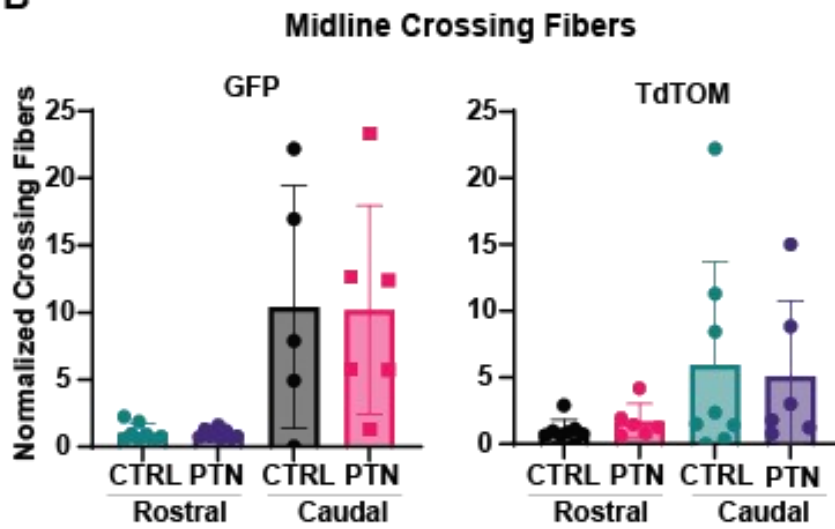
A**B**

Figure 8: Comparison of midline crossing fibres from PTN and PBS treated rats following the contusion SCI.

(A) Images outlining the midline crossing fibres that were quantified to measure neurite outgrowth. The white solid lines outline the spinal grey matter. The white dotted lines outline the CST and central canal. On the enlarged images, the white arrowheads point to examples of midline crossing fibres. (B) Midline crossing CST fibres traced with AAV9-GFP and tdTom in the spinal grey matter were quantified in each rat and normalized to the number of CST fibres traced in each rat. PTN and PBS-treated rats showed no significant differences in the amount of midline crossing CST fibres both rostral and caudal to the injury site.

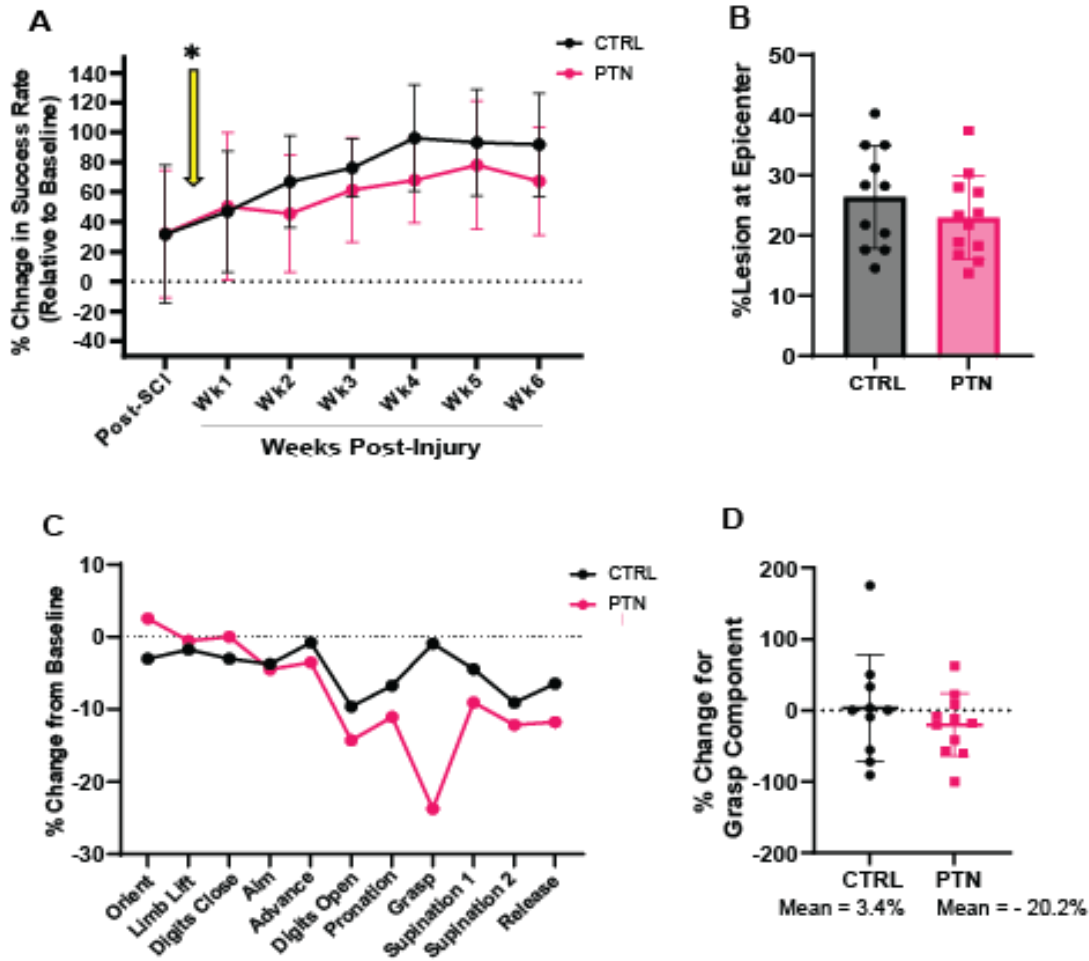


Figure 9: Outcome of rats with a DLQ SCI treated with PTN and SPG training compared to PBS-treated rats with SPG training.

(A) The SPG score of rats following the SCI and then 1-6 weeks following the spinal injection of either PTN or PBS. The yellow arrow with an * indicated a 13-day gap between when the SCI was given to when the spinal injections were given. The SPG score was normalized to the highest SPG success score obtained pre-SCI. Rats treated with PTN recovered slightly less than PBS-treated rats in the SPG task. (B) There was no significant difference in the area of lesioned tissue at the SCI epicentre between PBS- and PTN-treated rats.

(C) Using high-speed video recordings, specific components of the SPG task were scored at baseline before SCI and post-SCI at the end of SPG training. The data is presented as the percentage change in performance from the baseline scores. PTN-treated rats performed more poorly in all components of the SPG task following the 'aim' component. (D) Percent change values for PTN and CTRL rats for the grasping component of the high-speed analysis. The mean for the CTRL group is 3.4% and the mean for PTN group is -20.2%.

Figure 10: Analysis of GFP and tdTom tracing intensity and synaptic density using bassoon IHC.

(A) The intensity of AAV9 tracers and bassoon IHC were compared between the ipsilesional and contralesional sides at 3 defined areas (VH, IH, and DH) in the grey matter of the spinal cord (the grey matter and defined regions of the spinal cord are outlined in yellow). The dotted line labelled '1' is the horizontal line drawn across the grey matter at the most ventral and midline part of the grey matter. The dotted line labelled '2' is the horizontal line drawn across the grey matter when the CST begins to diverge from the grey matter. AAV9-GFP and tdTom are in green and red, respectively. The blue tint in the spinal grey matter is the bassoon stain. The intensity of each tracer and stain was analyzed rostral to the SCI, at the spinal injection site, and caudal to the injection site. The ratio of the AAV9 tracer and bassoon staining intensity on the ipsilesional side to the contralesional side are plotted from graphs B-G. A ratio greater than 1 indicates that the intensity of the tracer is greater on the ipsilesional side (the side with GFP traced CST). GFP tracing was significantly less in PTN-treated rats in the DH caudal to the injection site compared to CTRL rats (G). The intensity ratios for bassoon IHC in the VH caudal to the injection site was significantly less than PBS-treated rats (J). * $P \leq 0.05$, error bars show the standard deviation.

Bibliography

1. Noonan, V. K. *et al.* Incidence and Prevalence of Spinal Cord Injury in Canada: A National Perspective. *NED* **38**, 219–226 (2012).
2. Singh, A., Tetreault, L., Kalsi-Ryan, S., Nouri, A. & Fehlings, M. G. Global prevalence and incidence of traumatic spinal cord injury. *Clin Epidemiol* **6**, 309–331 (2014).
3. Pickett, W., Simpson, K., Walker, J. & Brison, R. J. Traumatic Spinal Cord Injury in Ontario, Canada. *Journal of Trauma and Acute Care Surgery* **55**, 1070–1076 (2003).
4. Alizadeh, A., Dyck, S. M. & Karimi-Abdolrezaee, S. Traumatic Spinal Cord Injury: An Overview of Pathophysiology, Models and Acute Injury Mechanisms. *Front Neurol* **10**, 282 (2019).
5. Kwon, B. K., Tetzlaff, W., Grauer, J. N., Beiner, J. & Vaccaro, A. R. Pathophysiology and pharmacologic treatment of acute spinal cord injury. *The Spine Journal* **4**, 451–464 (2004).
6. Waller, A. V. & Owen, R. XX. Experiments on the section of the glossopharyngeal and hypoglossal nerves of the frog, and observations of the alterations produced thereby in the structure of their primitive fibres. *Philosophical Transactions of the Royal Society of London* **140**, 423–429 (1850).
7. Raivich, G. *et al.* The AP-1 Transcription Factor c-Jun Is Required for Efficient Axonal Regeneration. *Neuron* **43**, 57–67 (2004).
8. Seiffers, R., Allchorne, A. J. & Woolf, C. J. The transcription factor ATF-3 promotes neurite outgrowth. *Molecular and Cellular Neuroscience* **32**, 143–154 (2006).
9. Tetzlaff, W., Alexander, S. W., Miller, F. D. & Bisby, M. A. Response of facial and rubrospinal neurons to axotomy: changes in mRNA expression for cytoskeletal proteins and GAP-43. *J. Neurosci.* **11**, 2528–2544 (1991).

10. Vargas, M. E. & Barres, B. A. Why is Wallerian degeneration in the CNS so slow? *Annu Rev Neurosci* **30**, 153–179 (2007).
11. George, R. & Griffin, J. W. Delayed Macrophage Responses and Myelin Clearance during Wallerian Degeneration in the Central Nervous System: The Dorsal Radiculotomy Model. *Experimental Neurology* **129**, 225–236 (1994).
12. Chen, M. S. *et al.* Nogo-A is a myelin-associated neurite outgrowth inhibitor and an antigen for monoclonal antibody IN-1. *Nature* **403**, 434–439 (2000).
13. McKerracher, L. *et al.* Identification of myelin-associated glycoprotein as a major myelin-derived inhibitor of neurite growth. *Neuron* **13**, 805–811 (1994).
14. Wang, K. C. *et al.* Oligodendrocyte-myelin glycoprotein is a Nogo receptor ligand that inhibits neurite outgrowth. *Nature* **417**, 941–944 (2002).
15. Liu, B. P., Fournier, A., GrandPré, T. & Strittmatter, S. M. Myelin-Associated Glycoprotein as a Functional Ligand for the Nogo-66 Receptor. *Science* **297**, 1190–1193 (2002).
16. Fournier, A. E., GrandPre, T. & Strittmatter, S. M. Identification of a receptor mediating Nogo-66 inhibition of axonal regeneration. *Nature* **409**, 341–346 (2001).
17. Niederöst, B., Oertle, T., Fritsche, J., McKinney, R. A. & Bandtlow, C. E. Nogo-A and myelin-associated glycoprotein mediate neurite growth inhibition by antagonistic regulation of RhoA and Rac1. *J Neurosci* **22**, 10368–10376 (2002).
18. Leung, T., Manser, E., Tan, L. & Lim, L. A Novel Serine/Threonine Kinase Binding the Ras-related RhoA GTPase Which Translocates the Kinase to Peripheral Membranes (*). *Journal of Biological Chemistry* **270**, 29051–29054 (1995).
19. Nakagawa, O. *et al.* ROCK-I and ROCK-II, two isoforms of Rho-associated coiled-coil forming protein serine/threonine kinase in mice. *FEBS Letters* **392**, 189–193 (1996).

20. Endo, M. *et al.* Control of Growth Cone Motility and Morphology by LIM Kinase and Slingshot via Phosphorylation and Dephosphorylation of Cofilin. *J. Neurosci.* **23**, 2527–2537 (2003).
21. Lehmann, M. *et al.* Inactivation of Rho Signaling Pathway Promotes CNS Axon Regeneration. *J. Neurosci.* **19**, 7537–7547 (1999).
22. Lingor, P. *et al.* Inhibition of Rho kinase (ROCK) increases neurite outgrowth on chondroitin sulphate proteoglycan in vitro and axonal regeneration in the adult optic nerve in vivo. *J Neurochem* **103**, 181–189 (2007).
23. Mckeon, R. J., Höke, A. & Silver, J. Injury-Induced Proteoglycans Inhibit the Potential for Laminin-Mediated Axon Growth on Astrocytic Scars. *Experimental Neurology* **136**, 32–43 (1995).
24. Bovolenta, P., Wandosell, F. & Nieto-Sampedro, M. Chapter 31: CNS glial scar tissue: a source of molecules which inhibit central neurite outgrowth. in *Progress in Brain Research* (eds. Yu, A. C. H., Hertz, L., Norenberg, M. D., Syková, E. & Waxman, S. G.) vol. 94 367–379 (Elsevier, 1992).
25. Nicaise, A. M. *et al.* The role of neural stem cells in regulating glial scar formation and repair. *Cell Tissue Res* **387**, 399–414 (2022).
26. Faulkner, J. R. *et al.* Reactive Astrocytes Protect Tissue and Preserve Function after Spinal Cord Injury. *J. Neurosci.* **24**, 2143–2155 (2004).
27. Yang, T., Dai, Y., Chen, G. & Cui, S. Dissecting the Dual Role of the Glial Scar and Scar-Forming Astrocytes in Spinal Cord Injury. *Frontiers in Cellular Neuroscience* **14**, (2020).

28. Jones, L. L., Margolis, R. U. & Tuszynski, M. H. The chondroitin sulfate proteoglycans neurocan, brevican, phosphacan, and versican are differentially regulated following spinal cord injury. *Experimental Neurology* **182**, 399–411 (2003).
29. Shen, Y. *et al.* PTP σ Is a Receptor for Chondroitin Sulfate Proteoglycan, an Inhibitor of Neural Regeneration. *Science* **326**, 592–596 (2009).
30. Fisher, D. *et al.* Leukocyte Common Antigen-Related Phosphatase Is a Functional Receptor for Chondroitin Sulfate Proteoglycan Axon Growth Inhibitors. *J. Neurosci.* **31**, 14051–14066 (2011).
31. Dickendesher, T. L. *et al.* NgR1 and NgR3 are receptors for chondroitin sulfate proteoglycans. *Nature Neuroscience* **15**, 703–712 (2012).
32. Galtrey, C. M., Kwok, J. C. F., Carulli, D., Rhodes, K. E. & Fawcett, J. W. Distribution and synthesis of extracellular matrix proteoglycans, hyaluronan, link proteins and tenascin-R in the rat spinal cord. *European Journal of Neuroscience* **27**, 1373–1390 (2008).
33. Avram, S., Shaposhnikov, S., Buiu, C. & Mernea, M. Chondroitin Sulfate Proteoglycans: Structure-Function Relationship with Implication in Neural Development and Brain Disorders. *BioMed Research International* **2014**, e642798 (2014).
34. Celio, M. R., Spreafico, R., De Biasi, S. & Vitellaro-Zuccarello, L. Perineuronal nets: past and present. *Trends in Neurosciences* **21**, 510–515 (1998).
35. Cai, D. *et al.* Neuronal Cyclic AMP Controls the Developmental Loss in Ability of Axons to Regenerate. *J. Neurosci.* **21**, 4731–4739 (2001).
36. Park, K. K. *et al.* Promoting Axon Regeneration in the Adult CNS by Modulation of the PTEN/mTOR Pathway. *Science* **322**, 963–966 (2008).

37. Liu, K. *et al.* PTEN deletion enhances the regenerative ability of adult corticospinal neurons. *Nature Neuroscience* **13**, 1075–1081 (2010).
38. Qiu, J. *et al.* Spinal Axon Regeneration Induced by Elevation of Cyclic AMP. *Neuron* **34**, 895–903 (2002).
39. Pearse, D. D. *et al.* cAMP and Schwann cells promote axonal growth and functional recovery after spinal cord injury. *Nature Medicine* **10**, 610–616 (2004).
40. Nikulina, E., Tidwell, J. L., Dai, H. N., Bregman, B. S. & Filbin, M. T. The phosphodiesterase inhibitor rolipram delivered after a spinal cord lesion promotes axonal regeneration and functional recovery. *PNAS* **101**, 8786–8790 (2004).
41. Lau, B. Y. B., Fogerson, S. M., Walsh, R. B. & Morgan, J. R. Cyclic AMP promotes axon regeneration, lesion repair and neuronal survival in lampreys after spinal cord injury. *Experimental Neurology* **250**, 31–42 (2013).
42. Blight, A. R. Delayed Demyelination and Macrophage Invasion: A Candidate for Secondary Cell Damage in Spinal Cord Injury. *Central Nervous System Trauma* **2**, 299–315 (1985).
43. Felts, P. A., Baker, T. A. & Smith, K. J. Conduction in Segmentally Demyelinated Mammalian Central Axons. *J. Neurosci.* **17**, 7267–7277 (1997).
44. Jeffery, N. D. & Blakemore, W. F. Locomotor deficits induced by experimental spinal cord demyelination are abolished by spontaneous remyelination. *Brain* **120**, 27–37 (1997).
45. James, N. D. *et al.* Conduction Failure following Spinal Cord Injury: Functional and Anatomical Changes from Acute to Chronic Stages. *J. Neurosci.* **31**, 18543–18555 (2011).
46. Trapp, B. D. & Stys, P. K. Virtual hypoxia and chronic necrosis of demyelinated axons in multiple sclerosis. *The Lancet Neurology* **8**, 280–291 (2009).

47. Waxman, S. G. Axonal conduction and injury in multiple sclerosis: the role of sodium channels. *Nat Rev Neurosci* **7**, 932–941 (2006).
48. Irvine, K. A. & Blakemore, W. F. Remyelination protects axons from demyelination-associated axon degeneration. *Brain* **131**, 1464–1477 (2008).
49. Nguyen, T. *et al.* Axonal Protective Effects of the Myelin-Associated Glycoprotein. *J. Neurosci.* **29**, 630–637 (2009).
50. Karimi-Abdolrezaee, S., Eftekharpour, E., Wang, J., Morshead, C. M. & Fehlings, M. G. Delayed Transplantation of Adult Neural Precursor Cells Promotes Remyelination and Functional Neurological Recovery after Spinal Cord Injury. *J. Neurosci.* **26**, 3377–3389 (2006).
51. Simonen, M. *et al.* Systemic Deletion of the Myelin-Associated Outgrowth Inhibitor Nogo-A Improves Regenerative and Plastic Responses after Spinal Cord Injury. *Neuron* **38**, 201–211 (2003).
52. GrandPré, T., Li, S. & Strittmatter, S. M. Nogo-66 receptor antagonist peptide promotes axonal regeneration. *Nature* **417**, 547–551 (2002).
53. Bradbury, E. J. *et al.* Chondroitinase ABC promotes functional recovery after spinal cord injury. *Nature* **416**, 636–640 (2002).
54. Rosenzweig, E. S. *et al.* Chondroitinase improves anatomical and functional outcomes after primate spinal cord injury. *Nature Neuroscience* **22**, 1269–1275 (2019).
55. James, N. D. *et al.* Chondroitinase gene therapy improves upper limb function following cervical contusion injury. *Exp Neurol* **271**, 131–135 (2015).
56. Daneshjou, S., Dabirmanesh, B., Rahimi, F. & Khajeh, K. Porous silicon nanoparticle as a stabilizing support for chondroitinase. *Int J Biol Macromol* **94**, 852–858 (2017).

57. Muir, E., De Winter, F., Verhaagen, J. & Fawcett, J. Recent advances in the therapeutic uses of chondroitinase ABC. *Exp Neurol* **321**, 113032 (2019).
58. Fouad, K. *et al.* Combining Schwann Cell Bridges and Olfactory-Ensheathing Glia Grafts with Chondroitinase Promotes Locomotor Recovery after Complete Transection of the Spinal Cord. *J. Neurosci.* **25**, 1169–1178 (2005).
59. Barraud, P. *et al.* Neural crest origin of olfactory ensheathing glia. *Proceedings of the National Academy of Sciences* **107**, 21040–21045 (2010).
60. Hubel, D. H. & Wiesel, T. N. The period of susceptibility to the physiological effects of unilateral eye closure in kittens. *The Journal of Physiology* **206**, 419–436 (1970).
61. Hebb, D. O. Organization of behavior. *J. Clin. Psychol* **6**, 335–307.
62. Fouad, K., Pedersen, V., Schwab, M. E. & Brösamle, C. Cervical sprouting of corticospinal fibers after thoracic spinal cord injury accompanies shifts in evoked motor responses. *Curr Biol* **11**, 1766–1770 (2001).
63. Wu, C. W.-H. & Kaas, J. H. Reorganization in Primary Motor Cortex of Primates with Long-Standing Therapeutic Amputations. *J. Neurosci.* **19**, 7679–7697 (1999).
64. Girgis, J. *et al.* Reaching training in rats with spinal cord injury promotes plasticity and task specific recovery. *Brain* **130**, 2993–3003 (2007).
65. Fouad, K., Metz, G. A. S., Merkler, D., Dietz, V. & Schwab, M. E. Treadmill training in incomplete spinal cord injured rats. *Behavioural Brain Research* **115**, 107–113 (2000).
66. Courtine, G. *et al.* Recovery of supraspinal control of stepping via indirect propriospinal relay connections after spinal cord injury. *Nat Med* **14**, 69–74 (2008).
67. Eidelberg, E., Story, J. L., Walden, J. G. & Meyer, B. L. Anatomical correlates of return of locomotor function after partial spinal cord lesions in cats. *Exp Brain Res* **42**, 81–88 (1981).

68. Little, J. W., Harris, R. M. & Sohlberg, R. C. Locomotor recovery following subtotal spinal cord lesions in a rat model. *Neuroscience Letters* **87**, 189–194 (1988).
69. Helgren, M. E. & Goldberger, M. E. The Recovery of Postural Reflexes and Locomotion Following Low Thoracic Hemisection in Adult Cats Involves Compensation by Undamaged Primary Afferent Pathways. *Experimental Neurology* **123**, 17–34 (1993).
70. Gómez-Pinilla, F. *et al.* BDNF and learning: Evidence that instrumental training promotes learning within the spinal cord by up-regulating BDNF expression. *Neuroscience* **148**, 893–906 (2007).
71. Krajacic, A., Ghosh, M., Puentes, R., Pearse, D. D. & Fouad, K. Advantages of delaying the onset of rehabilitative reaching training in rats with incomplete spinal cord injury. *Eur J Neurosci* **29**, 641–651 (2009).
72. Duan, R. *et al.* Clinical Benefit of Rehabilitation Training in Spinal Cord Injury: A Systematic Review and Meta-Analysis. *Spine* **46**, E398 (2021).
73. Ho, C. H. *et al.* Functional Electrical Stimulation and Spinal Cord Injury. *Phys Med Rehabil Clin N Am* **25**, 631–ix (2014).
74. Wang, A. *et al.* Fastigial nucleus electrostimulation promotes axonal regeneration after experimental stroke via cAMP/PKA pathway. *Neuroscience Letters* **699**, 177–183 (2019).
75. Wenjin, W. *et al.* Electrical Stimulation Promotes BDNF Expression in Spinal Cord Neurons Through Ca²⁺- and Erk-Dependent Signaling Pathways. *Cell Mol Neurobiol* **31**, 459–467 (2011).
76. García-Álías, G., Barkhuysen, S., Buckle, M. & Fawcett, J. W. Chondroitinase ABC treatment opens a window of opportunity for task-specific rehabilitation. *Nature Neuroscience* **12**, 1145–1151 (2009).

77. Rauvala, H. An 18-kd heparin-binding protein of developing brain that is distinct from fibroblast growth factors. *The EMBO Journal* **8**, 2933–2941 (1989).
78. Li, Y. S. *et al.* Cloning and expression of a developmentally regulated protein that induces mitogenic and neurite outgrowth activity. *Science* **250**, 1690–1694 (1990).
79. Krellman, J. W., Ruiz, H. H., Marciano, V. A., Mondrow, B. & Croll, S. D. Behavioral and Neuroanatomical Abnormalities in Pleiotrophin Knockout Mice. *PLOS ONE* **9**, e100597 (2014).
80. Gombash, S. E. *et al.* Striatal Pleiotrophin Overexpression Provides Functional and Morphological Neuroprotection in the 6-Hydroxydopamine Model. *Mol Ther* **20**, 544–554 (2012).
81. Yanagisawa, H., Komuta, Y., Kawano, H., Toyoda, M. & Sango, K. Pleiotrophin induces neurite outgrowth and up-regulates growth-associated protein (GAP)-43 mRNA through the ALK/GSK3 β / β -catenin signaling in developing mouse neurons. *Neuroscience Research* **66**, 111–116 (2010).
82. Rauvala, H. *et al.* Expression of HB-GAM (heparin-binding growth-associated molecules) in the pathways of developing axonal processes in vivo and neurite outgrowth in vitro induced by HB-GAM. *Developmental Brain Research* **79**, 157–176 (1994).
83. Merenmies, J. & Rauvala, H. Molecular cloning of the 18-kDa growth-associated protein of developing brain. *J. Biol. Chem.* **265**, 16721–16724 (1990).
84. Wang, X. Pleiotrophin: Activity and Mechanism. *Adv Clin Chem* **98**, 51–89 (2020).
85. Wanaka, A., Carroll, S. L. & Milbrandt, J. Developmentally regulated expression of pleiotrophin, a novel heparin binding growth factor, in the nervous system of the rat. *Developmental Brain Research* **72**, 133–144 (1993).

86. Nikolakopoulou, A. M. *et al.* Pericyte loss leads to circulatory failure and pleiotrophin depletion causing neuron loss. *Nat Neurosci* **22**, 1089–1098 (2019).
87. Gramage, E. *et al.* The neurotrophic factor pleiotrophin modulates amphetamine-seeking behaviour and amphetamine-induced neurotoxic effects: evidence from pleiotrophin knockout mice. *Addiction Biology* **15**, 403–412 (2010).
88. Shi, Y. *et al.* Tumour-associated macrophages secrete pleiotrophin to promote PTPRZ1 signalling in glioblastoma stem cells for tumour growth. *Nat Commun* **8**, 15080 (2017).
89. Yeh, H.-J., He, Y. Y., Xu, J., Hsu, C. Y. & Deuel, T. F. Upregulation of Pleiotrophin Gene Expression in Developing Microvasculature, Macrophages, and Astrocytes after Acute Ischemic Brain Injury. *J. Neurosci.* **18**, 3699–3707 (1998).
90. Wang, Y.-T. *et al.* Upregulation of heparin-binding growth-associated molecule after spinal cord injury in adult rats. *Acta Pharmacol Sin* **25**, 611–616 (2004).
91. Paveliev, M. *et al.* HB-GAM (pleiotrophin) reverses inhibition of neural regeneration by the CNS extracellular matrix. *Scientific Reports* **6**, 33916 (2016).
92. Kuleskaya, N. *et al.* Heparin-Binding Growth-Associated Molecule (Pleiotrophin) Affects Sensory Signaling and Selected Motor Functions in Mouse Model of Anatomically Incomplete Cervical Spinal Cord Injury. *Frontiers in Neurology* **12**, (2021).
93. Motegi, A., Fujimoto, J., Kotani, M., Sakuraba, H. & Yamamoto, T. ALK receptor tyrosine kinase promotes cell growth and neurite outgrowth. *J Cell Sci* **117**, 3319–3329 (2004).
94. Gupta, S. J., Churchward, M. A., Todd, K. G. & Winship, I. R. Pleiotrophin signals through ALK receptor to enhance growth of neurons in the presence of inhibitory CSPGs. 2022.04.01.486745 Preprint at <https://doi.org/10.1101/2022.04.01.486745> (2022).

95. Barritt, A. W. *et al.* Chondroitinase ABC Promotes Sprouting of Intact and Injured Spinal Systems after Spinal Cord Injury. *J. Neurosci.* **26**, 10856–10867 (2006).
96. Tester, N. J., Plaas, A. H. & Howland, D. R. Effect of body temperature on chondroitinase ABC's ability to cleave chondroitin sulfate glycosaminoglycans. *Journal of Neuroscience Research* **85**, 1110–1118 (2007).
97. Weidner, N., Ner, A., Salimi, N. & Tuszynski, M. H. Spontaneous corticospinal axonal plasticity and functional recovery after adult central nervous system injury. *PNAS* **98**, 3513–3518 (2001).
98. Bareyre, F. M. *et al.* The injured spinal cord spontaneously forms a new intraspinal circuit in adult rats. *Nat Neurosci* **7**, 269–277 (2004).
99. Raineteau, O., Fouad, K., Bareyre, F. M. & Schwab, M. E. Reorganization of descending motor tracts in the rat spinal cord. *European Journal of Neuroscience* **16**, 1761–1771 (2002).
100. Omoto, S., Ueno, M., Mochio, S. & Yamashita, T. Corticospinal tract fibers cross the ephrin-B3-negative part of the midline of the spinal cord after brain injury. *Neuroscience Research* **69**, 187–195 (2011).
101. Sato, T., Nakamura, Y., Takeda, A. & Ueno, M. Lesion Area in the Cerebral Cortex Determines the Patterns of Axon Rewiring of Motor and Sensory Corticospinal Tracts After Stroke. *Front Neurosci* **15**, 737034 (2021).
102. Starkey, M. L., Bartus, K., Barritt, A. W. & Bradbury, E. J. Chondroitinase ABC promotes compensatory sprouting of the intact corticospinal tract and recovery of forelimb function following unilateral pyramidotomy in adult mice. *European Journal of Neuroscience* **36**, 3665–3678 (2012).

103. Lang, C., Bradley, P. M., Jacobi, A., Kerschensteiner, M. & Bareyre, F. M. STAT3 promotes corticospinal remodelling and functional recovery after spinal cord injury. *EMBO Rep* **14**, 931–937 (2013).
104. Wang, D., Ichiyama, R. M., Zhao, R., Andrews, M. R. & Fawcett, J. W. Chondroitinase Combined with Rehabilitation Promotes Recovery of Forelimb Function in Rats with Chronic Spinal Cord Injury. *J. Neurosci.* **31**, 9332–9344 (2011).
105. Tom, V. J., Kadakia, R., Santi, L. & Houlé, J. D. Administration of Chondroitinase ABC Rostral or Caudal to a Spinal Cord Injury Site Promotes Anatomical but Not Functional Plasticity. *Journal of Neurotrauma* **26**, 2323–2333 (2009).
106. Sotocina, S. G. *et al.* The Rat Grimace Scale: A Partially Automated Method for Quantifying Pain in the Laboratory Rat via Facial Expressions. *Mol Pain* **7**, 1744-8069-7–55 (2011).
107. Torres-Espín, A. *et al.* Eliciting inflammation enables successful rehabilitative training in chronic spinal cord injury. *Brain* **141**, 1946–1962 (2018).
108. Schmidt, E., Raposo, P., Vavrek, R. & Fouad, K. Inducing inflammation following subacute spinal cord injury in female rats: A double-edged sword to promote motor recovery. *Brain, Behavior, and Immunity* **93**, 55–65 (2021).
109. Schmidt, E. K. A., Raposo, P. J. F., Torres-Espin, A., Fenrich, K. K. & Fouad, K. Beyond the lesion site: minocycline augments inflammation and anxiety-like behavior following SCI in rats through action on the gut microbiota. *J Neuroinflammation* **18**, 1–16 (2021).
110. Fonoff, E. T. *et al.* Functional mapping of the motor cortex of the rat using transdural electrical stimulation. *Behavioural Brain Research* **202**, 138–141 (2009).

111. Metz, G. A. & Whishaw, I. Q. Cortical and subcortical lesions impair skilled walking in the ladder rung walking test: a new task to evaluate fore- and hindlimb stepping, placing, and coordination. *Journal of Neuroscience Methods* **115**, 169–179 (2002).
112. Torres-Espín, A., Forero, J., Schmidt, E. K. A., Fouad, K. & Fenrich, K. K. A motorized pellet dispenser to deliver high intensity training of the single pellet reaching and grasping task in rats. *Behavioural Brain Research* **336**, 67–76 (2018).
113. Whishaw, I. Q., Whishaw, P. & Gorny, B. The Structure of Skilled Forelimb Reaching in the Rat: A Movement Rating Scale. *J Vis Exp* 816 (2008) doi:10.3791/816.
114. Dieck, S. *et al.* Bassoon, a Novel Zinc-finger CAG/Glutamine-repeat Protein Selectively Localized at the Active Zone of Presynaptic Nerve Terminals. *Journal of Cell Biology* **142**, 499–509 (1998).
115. Sholl, D. A. Dendritic organization in the neurons of the visual and motor cortices of the cat. *J Anat* **87**, 387-406.1 (1953).
116. Powell, S. K. & Kleinman, H. K. Neuronal laminins and their cellular receptors. *The International Journal of Biochemistry & Cell Biology* **29**, 401–414 (1997).
117. Bertram, S. *et al.* Pleiotrophin increases neurite length and number of spiral ganglion neurons in vitro. *Exp Brain Res* **237**, 2983–2993 (2019).
118. Snow, D. M., Brown, E. M. & Letourneau, P. C. Growth Cone Behavior in the Presence of Soluble Chondroitin Sulfate Proteoglycan (cspg), Compared to Behavior on Cspg Bound to Laminin or Fibronectin. *International Journal of Developmental Neuroscience* **14**, 331–349 (1996).

119. Kjell, J. & Götz, M. Filling the Gaps – A Call for Comprehensive Analysis of Extracellular Matrix of the Glial Scar in Region- and Injury-Specific Contexts. *Front Cell Neurosci* **14**, 32 (2020).
120. Day, P. *et al.* Targeting chondroitinase ABC to axons enhances the ability of chondroitinase to promote neurite outgrowth and sprouting. *PLOS ONE* **15**, e0221851 (2020).
121. Maikos, J. T., Elias, R. A. I. & Shreiber, D. I. Mechanical Properties of Dura Mater from the Rat Brain and Spinal Cord. *Journal of Neurotrauma* **25**, 38–51 (2008).
122. Ichihara, K. *et al.* Gray Matter of the Bovine Cervical Spinal Cord is Mechanically More Rigid and Fragile than the White Matter. *Journal of Neurotrauma* **18**, 361–367 (2001).
123. Okada, S. The pathophysiological role of acute inflammation after spinal cord injury. *Inflamm Regen* **36**, 20 (2016).
124. Okada, S. *et al.* The role of cytokine signaling in pathophysiology for spinal cord injury. *Inflammation and Regeneration* **28**, 440–446 (2008).
125. Fernández-Calle, R. *et al.* Pleiotrophin regulates microglia-mediated neuroinflammation. *J Neuroinflammation* **14**, 1–10 (2017).
126. Pufe, T., Bartscher, M., Petersen, W., Tillmann, B. & Mentlein, R. Expression of pleiotrophin, an embryonic growth and differentiation factor, in rheumatoid arthritis. *Arthritis Rheum* **48**, 660–667 (2003).
127. Lu, K. V. *et al.* Differential Induction of Glioblastoma Migration and Growth by Two Forms of Pleiotrophin*. *Journal of Biological Chemistry* **280**, 26953–26964 (2005).

128. Herradón, G. & Pérez-García, C. Targeting midkine and pleiotrophin signalling pathways in addiction and neurodegenerative disorders: recent progress and perspectives. *British Journal of Pharmacology* **171**, 837–848 (2014).
129. Muramatsu, T. Midkine and Pleiotrophin: Two Related Proteins Involved in Development, Survival, Inflammation and Tumorigenesis. *The Journal of Biochemistry* **132**, 359–371 (2002).
130. Sorrelle, N., Dominguez, A. T. A. & Brekken, R. A. From top to bottom: midkine and pleiotrophin as emerging players in immune regulation. *Journal of Leukocyte Biology* **102**, 277–286 (2017).
131. Qin, L. *et al.* NADPH Oxidase Mediates Lipopolysaccharide-induced Neurotoxicity and Proinflammatory Gene Expression in Activated Microglia *. *Journal of Biological Chemistry* **279**, 1415–1421 (2004).
132. Zhang, A.-L. *et al.* Decreased GABA immunoreactivity in spinal cord dorsal horn neurons after transient spinal cord ischemia in the rat. *Brain Research* **656**, 187–190 (1994).
133. Gwak, Y. S., Nam, T. S., Paik, K. S., Hulsebosch, C. E. & Leem, J. W. Attenuation of mechanical hyperalgesia following spinal cord injury by administration of antibodies to nerve growth factor in the rat. *Neuroscience Letters* **336**, 117–120 (2003).
134. Lipachev, N. *et al.* Quantitative changes in perineuronal nets in development and posttraumatic condition. *J Mol Hist* **50**, 203–216 (2019).
135. Wang, D. & Fawcett, J. The perineuronal net and the control of CNS plasticity. *Cell Tissue Res* **349**, 147–160 (2012).
136. Tehranipour, M. & Moghimi, A. Neuroprotective Effects of Testosterone on Regenerating Spinal Cord Motoneurons in Rats. *Journal of Motor Behavior* **42**, 151–155 (2010).

137. Bagetta, G. *et al.* Estradiol reduces cytochrome c translocation and minimizes hippocampal damage caused by transient global ischemia in rat. *Neurosci Lett* **368**, 87–91 (2004).
138. Schumacher, M., Guennoun, R., Stein, D. G. & De Nicola, A. F. Progesterone: Therapeutic opportunities for neuroprotection and myelin repair. *Pharmacology & Therapeutics* **116**, 77–106 (2007).
139. Datto, J. P. *et al.* Female Rats Demonstrate Improved Locomotor Recovery and Greater Preservation of White and Gray Matter after Traumatic Spinal Cord Injury Compared to Males. *J Neurotrauma* **32**, 1146–1157 (2015).
140. Becker, J. B., Prendergast, B. J. & Liang, J. W. Female rats are not more variable than male rats: a meta-analysis of neuroscience studies. *Biol Sex Differ* **7**, 34 (2016).
141. Samantaray, S. *et al.* Neuroprotective efficacy of estrogen in experimental spinal cord injury in rats. *Annals of the New York Academy of Sciences* **1199**, 90–94 (2010).
142. Cornez, G., Haar, S. M. ter, Cornil, C. A. & Balthazart, J. Anatomically Discrete Sex Differences in Neuroplasticity in Zebra Finches as Reflected by Perineuronal Nets. *PLOS ONE* **10**, e0123199 (2015).
143. Zhang, N. *et al.* Hypothalamic Perineuronal Nets Are Regulated by Sex and Dietary Interventions. *Frontiers in Physiology* **12**, (2021).
144. Griffiths, B. B., Madden, A. M. K., Edwards, K. A., Zup, S. L. & Sary, C. M. Age-dependent sexual dimorphism in hippocampal cornu ammonis-1 perineuronal net expression in rats. *Brain and Behavior* **9**, e01265 (2019).
145. McCarthy, M. M. Sex differences in neuroimmunity as an inherent risk factor. *Neuropsychopharmacol* **44**, 38–44 (2019).

146. Arnold, A. Organizational and activational effects of sex steroids on brain and behavior: A reanalysis. *Hormones and Behavior* **19**, 469–498 (1985).
147. Forger, N. G. The organizational hypothesis and final common pathways: Sexual differentiation of the spinal cord and peripheral nervous system. *Hormones and Behavior* **55**, 605–610 (2009).
148. Späni, C. B., Braun, D. J. & Van Eldik, L. J. Sex-related responses after traumatic brain injury: Considerations for preclinical modeling. *Frontiers in Neuroendocrinology* **50**, 52–66 (2018).
149. Jadavji, N. M. & Metz, G. A. Sex differences in skilled movement in response to restraint stress and recovery from stress. *Behavioural Brain Research* **195**, 251–259 (2008).
150. Schrimsher, G. W. & Reier, P. J. Forelimb Motor Performance Following Dorsal Column, Dorsolateral Funiculi, or Ventrolateral Funiculi Lesions of the Cervical Spinal Cord in the Rat. *Experimental Neurology* **120**, 264–276 (1993).
151. McKenna, J. E., Prusky, G. T. & Whishaw, I. Q. Cervical motoneuron topography reflects the proximodistal organization of muscles and movements of the rat forelimb: A retrograde carbocyanine dye analysis. *Journal of Comparative Neurology* **419**, 286–296 (2000).
152. Tang, X., Davies, J. E. & Davies, S. J. A. Changes in distribution, cell associations, and protein expression levels of NG2, neurocan, phosphacan, brevican, versican V2, and tenascin-C during acute to chronic maturation of spinal cord scar tissue. *Journal of Neuroscience Research* **71**, 427–444 (2003).
153. Harding, E. K., Fung, S. W. & Bonin, R. P. Insights Into Spinal Dorsal Horn Circuit Function and Dysfunction Using Optical Approaches. *Frontiers in Neural Circuits* **14**, (2020).

154. Hargreaves, K., Dubner, R., Brown, F., Flores, C. & Joris, J. A new and sensitive method for measuring thermal nociception in cutaneous hyperalgesia. *Pain* **32**, 77–88 (1988).
155. Espejo, E. Structure of the rat's behaviour in the hot plate test. *Behavioural Brain Research* **56**, 171–176 (1993).
156. McKenna, J. E. & Wishaw, I. Q. Complete Compensation in Skilled Reaching Success with Associated Impairments in Limb Synergies, after Dorsal Column Lesion in the Rat. *J. Neurosci.* **19**, 1885–1894 (1999).
157. Fouad, K., Ng, C. & Basso, D. M. Behavioral testing in animal models of spinal cord injury. *Experimental Neurology* **333**, 113410 (2020).
158. Galtrey, C. M., Asher, R. A., Nothias, F. & Fawcett, J. W. Promoting plasticity in the spinal cord with chondroitinase improves functional recovery after peripheral nerve repair. *Brain* **130**, 926–939 (2007).
159. Irvine, S. F. & Kwok, J. C. F. Perineuronal Nets in Spinal Motoneurons: Chondroitin Sulphate Proteoglycan around Alpha Motoneurons. *Int J Mol Sci* **19**, (2018).
160. Stoltz, D., Silverstein, A., Huffman, E. & Alilain, W. Balancing Neuroprotection with Functional Recovery: The Potential Role of the PNN in Preventing Excitotoxicity after SCI. *The FASEB Journal* **33**, 557.11-557.11 (2019).
161. Meisner, J. G., Marsh, A. D. & Marsh, D. R. Loss of GABAergic Interneurons in Laminae I–III of the Spinal Cord Dorsal Horn Contributes to Reduced GABAergic Tone and Neuropathic Pain after Spinal Cord Injury. *Journal of Neurotrauma* **27**, 729–737 (2010).
162. Ferguson, A. R., Crown, E. D. & Grau, J. W. Nociceptive plasticity inhibits adaptive learning in the spinal cord. *Neuroscience* **141**, 421–431 (2006).

163. Hosseini, S. M. *et al.* Suppressing CSPG/LAR/PTP σ Axis Facilitates Neuronal Replacement and Synaptogenesis by Human Neural Precursor Grafts and Improves Recovery after Spinal Cord Injury. *J. Neurosci.* **42**, 3096–3121 (2022).
164. Snow, D. M., Steindler, D. A. & Silver, J. Molecular and cellular characterization of the glial roof plate of the spinal cord and optic tectum: A possible role for a proteoglycan in the development of an axon barrier. *Developmental Biology* **138**, 359–376 (1990).
165. Pulido, R., Serra-Pagès, C., Tang, M. & Streuli, M. The LAR/PTP delta/PTP sigma subfamily of transmembrane protein-tyrosine-phosphatases: multiple human LAR, PTP delta, and PTP sigma isoforms are expressed in a tissue-specific manner and associate with the LAR-interacting protein LIP.1. *Proc Natl Acad Sci U S A* **92**, 11686–11690 (1995).
166. Smart, I. & Leblond, C. P. Evidence for division and transformations of neuroglia cells in the mouse brain, as derived from radioautography after injection of thymidine-H3. *Journal of Comparative Neurology* **116**, 349–367 (1961).
167. Chakraborty, A., Ciciriello, A. J., Dumont, C. M. & Pearson, R. M. Nanoparticle-Based Delivery to Treat Spinal Cord Injury—a Mini-review. *AAPS PharmSciTech* **22**, 101 (2021).
168. Laabs, T., Carulli, D., Geller, H. M. & Fawcett, J. W. Chondroitin sulfate proteoglycans in neural development and regeneration. *Current Opinion in Neurobiology* **15**, 116–120 (2005).
169. Key, B. & Lah, G. J. Repulsive guidance molecule A (RGMa). *Cell Adh Migr* **6**, 85–90 (2012).
170. NIH NOT-OD-15-102.html. Consideration of Sex as a Biological Variable in NIH-funded Research. Available online at: <https://grants-nih.gov/login.ezproxy.library.ualberta.ca/grants/guide/notice-files/NOT-OD-15-102.html> (accessed July 5, 2022) (2015).

171. Fouad, K. *et al.* FAIR SCI Ahead: The Evolution of the Open Data Commons for Pre-Clinical Spinal Cord Injury Research. *Journal of Neurotrauma* **37**, 831–838 (2020).